# Bimetallic Reactivity. Synthesis of Bimetallic Complexes of Macrocyclic Binucleating Ligands Containing 6- and 4-Coordinate Sites and Their Reactivity with Dioxygen and Other Oxidants

**David G. McCollum,[†] Glenn P. A. Yap,[‡] Arnold L. Rheingold,[‡] and B. Bosnich*[,†]**

*Contribution from the Department of Chemistry, The University of Chicago, 5735 South Ellis Avenue, Chicago, Illinois 60637, and Department of Chemistry and Biochemistry, University of Delaware, Newark, Delaware 19716*

*Received August 21, 1995*[⊗]

**Abstract:** General methods are described for the synthesis of amine macrocyclic ligand systems which can contiguously accommodate two metals, one in a 6-coordinate site and the other in a 4-coordinate location. The amine complexes of the type $[M(\text{amine ligand})(H^+)_2]^{n+}$, where M is in the 6-coordinate site and the other site contains two protons, are obtained from the previously described imine complexes, $[M(\text{imine ligand})(H^+)_2]^{n+}$, by $BH_4^-$ reduction. The macrocyclic framework consists of two diamine links, one at each site. Ligands incorporating the trimethylenediamine (tn) and ethylenediamine (en) links were prepared, namely, the four ligands containing the tntn, tnen, entn, and enen combinations. Bimetallic complexes of the amine ligands are prepared under mild conditions from the monometallic complexes $[M(\text{amine ligand})(H^+)_2]^{n+}$ by addition of the second metal. The structures of these complexes were studied by $^1H$ NMR spectrometry and by X-ray diffraction. The monometallic imine complexes, $[Co^{II}(\text{imine ligand})(H^+)_2]^{2+}$, are oxidized to cobalt(III) complexes by ferrocinium ions ($fc^+$) when en links are present in the 6-coordinate site but this is not the case when tn is present in this site. All of the amine complexes, $[Co^{II}(\text{amine ligand})(H^+)_2]^{2+}$, are oxidized by $fc^+$ to give stable cobalt(III) complexes and it is concluded that the rigidity of the imine ligands prevents the ligand from adjusting to the stereochemical demands of cobalt(III) when the 6-coordinate site contains the larger tn link in the imine systems. This stereochemical impediment is relaxed in the more flexible amine systems. This effect is called mechanical coupling. Ferrocinium ion oxidation of the bimetallic amine complexes, $[Co^{II}(\text{amine ligand})Co^{II}Cl]^+$, leads only to the formation of the mixed oxidation state complexes, $[Co^{III}(\text{amine ligand})Co^{II}Cl]^{2+}$, where the cobalt(III) is in the 6-coordinate site. Unlike the imine dicobalt(II) complexes which are unreactive to dioxygen, the amine ligand dicobalt(II) complexes readily react with dioxygen to give the mixed oxidation state complexes, $[Co^{II}(\text{amine ligand})Co^{III}(Cl)(X)]^+$, where now the cobalt(III) ion occupies the 4-coordinate site. The inability to form stable dicobalt(III) complexes with these amine ligands, despite the fact that each site is capable of supporting the cobalt(III) states, is ascribed to various forms of coupling between the metals in the two sites. Three forms of coupling are considered and discussed; these are, mechanical coupling which refers to ligand constraints, through-space electrostatic interactions between metals, and through-bond coupling which refers to covalent interaction between the metals via the bridging ligands.

There are numerous examples of multimetallic proteins which employ the reducing power of several metals to transform substrates.[1] Of particular interest in the present context are, for example, the proteins hemerythrin[2] and ascorbate oxidase.[3] The former consists of two contiguous iron(II) atoms which upon exposure to dioxygen are oxidized to the diiron(III) state by reduction of the dioxygen to peroxide. The peroxide is bound to only one iron(III) atom suggesting that the two-electron reduction of dioxygen occurs by cooperative two-electron transfer, where one electron is transferred from each iron atom.

[†] The University of Chicago.

[‡] University of Delaware.

[⊗] Abstract published in *Advance ACS Abstracts,* February 1, 1996.

(1) Dinuclear Iron Proteins: (a) Howard, J. B.; Rees, D. C. *Adv. Protein Chem.* **1991**, *42*, 199−280. (b) Feig, A. L.; Lippard, S. J. *Chem. Rev.* **1994**, *94*, 759−805. (c) Rosenzweig, A. C.; Frederick, C. A.; Lippard, S. J.; Nordlund, P. *Nature* **1993**, *366*, 537−43. (d) Solomon, E. I.; Zhang, Y. *Acc. Chem. Res.* **1992**, *25*, 343−52. (e) Que, L., Jr.; True, A. E. *Prog. Inorg. Chem.* **1990**, *38*, 97−200. Cytochrome *c*: (f) Scott, M. J.; Zhang, H. H.; Lee, S. C.; Hedman, B.; Hodgson, K. O.; Holm, R. H. *J. Am. Chem. Soc.* **1995**, *117*, 568−69. (g) Karlin, K. D.; Nanthakumar, A.; Fox, S.; Murthy, N. N.; Ravi, N.; Huynh, B. H.; Orosz, R. D.; Day, E. P. *J. Am. Chem. Soc.* **1994**, *116*, 4753−63. (h) Varotsis, C.; Zhang, Y.; Appelman, E. H.; Babcock, G. T. *Proc. Natl. Acad. Sci., U.S.A.* **1993**, *90*, 237−41. (i) Babcock, G. T.; Wikström, M. *Nature* **1992**, *356*, 301−09. Multinuclear Copper Proteins: (j) Knowles, P. F.; Brown, R. D., III; Koenig, S. H.; Wang, S.; Scott, R. A.; McGuirl, M. A.; Brown, D. E.; Dooley, D. M. *Inorg. Chem.* **1995**, *34*, 3895−3902. (k) Kitajima, N.; Moro-oka, Y. *Chem. Rev.* **1994**, *94*, 737−57. l. Karlin, K. D.; Tyeklár, Z.; Zuberbühler, A. D. In *Bioinorganic Catalysis*; Reedijk, J., Ed.; Marcel Dekker, Inc.: New York, 1993; pp 261−315.

(2) Hemerythrin: (a) Stenkamp, R. E. *Chem. Rev.* **1994**, *94*, 715−27. (b) Wilkins, R. G. *Chem. Soc. Rev.* **1992**, 171−78. (c) Kitajima, N.; Tamura, N.; Tanaka, M.; Moro-oka, Y. *Inorg. Chem.* **1992**, *31*, 3342−43. (d) Mauerer, B.; Crane, J.; Schuler, J.; Wieghardt, K.; Nuber, B. *Angew. Chem., Int. Ed. Engl.* **1993**, *32*, 289−91. (e) Tolman, W. B.; Bino, A.; Lippard, S. J. *J. Am. Chem. Soc.* **1989**, *111*, 8522−23. (f) Nocek, J. M.; Kurtz, D. M., Jr.; Sage, J. T.; Xia, Y.-M.; Debrunner, P.; Shiemke, A. K.; Sanders-Loehr, J.; Loehr, T. M. *Biochemistry* **1988**, *27*, 1014−24.

(3) Ascorbate Oxidase: (a) Messerschmidt, A.; Luecke, H.; Huber, R. *J. Mol. Biol.* **1993**, *230*, 997−1014. (b) Messerschmidt, A.; Ladenstein, R.; Huber, R.; Bolognesi, M.; Avigliano, L.; Petruzelli, R.; Rossi, A.; Finazzi-Agró, A. *J. Mol. Biol.* **1992**, *224*, 179−205. (c) Messerschmidt, A.; Steigemann, W.; Huber, R.; Lang, G.; Kroneck, P. M. H. *Eur. J. Biochem.* **1992**, *209*, 597−602. (d) Messerschmidt, A.; Rossi, A.; Ladenstein, R.; Huber, R.; Bolognesi, M.; Gatti, G.; Marchesini, A.; Petruzelli, R.; Finazzo-Agró, A. *J. Mol. Biol.* **1989**, *206*, 513−29.

0002-7863/96/1518-1365$12.00/0 

In the case of ascorbate oxidase, four copper(I) atoms are involved in the four-electron reduction of dioxygen. Although it appears that the dioxygen is bound to two of the copper atoms, as a bridging Cu(II)−Cu(II) peroxide species, the other two copper atoms do not appear to bind dioxygen but rather serve to provide two electrons to the peroxide to generate water. Such behavior, where the substrate is bound and reduced by one or two metals and then is reduced further by other metals not directly bound to the substrate, has been difficult to reproduce in model systems.

We have recently developed a family of macrocyclic binucleating ligands of the type **1** which served to explore the factors

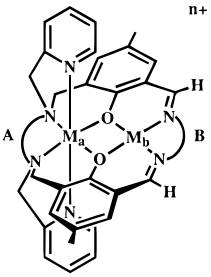

**1**

involved in cooperative bimetallic reduction of substrates.[4−8] The ligand was designed so that one metal, $M_a$, resided in a sexadentate site (closed-site) and the other metal, $M_b$, occupied a contiguous quadridentate site (open-site). The idea behind this design was the expectation that the substrate would bind to the open-site metal and be reduced by both of the metals. For example, as in the case of hemerythrin, it was considered possible that with appropriate ligand design and judicious choice of metals, dioxygen could bind to the open-site metal and be reduced to peroxide by the transfer of one electron from each metal. It is clear that such a system could be employed for 2-electron oxidative addition of substrates other than dioxygen. For example, $NO^+$ might be reduced to $NO^-$ by 2-electron oxidative addition. Further, because the approach is not restricted to the use of biologically known metals, ligand types, or structures, the necessary characteristics of the known biological functions are explored by a general, non-restrictive approach. In this way it was hoped to determine systematically the factors which allow for multielectron reduction of substrates by multimetallic systems.

In order to achieve this goal we were required to solve a number of synthetic and stereochemical problems with our systems. Among these were the synthesis of practical quantities of the ligands, the development of methods for the site-specific incorporation of the metals, an understanding of the relationship between the topological structure and chelate ring size (A and B), and the correlation between structure and redox properties of the metals. Many of these issues have been addressed previously[4−8] but there remained a perplexing relationship between the redox potentials of the metals and the ligand structure. In order to put these and other questions in context, we briefly outline the synthetic methods and other features of these systems.

The dialdehyde ligands **2** were isolated as their crystalline dilithio salts. Reaction of **2** with a divalent metal gives the monometallic complexes **3** which, upon isolation, can be cyclized with a diamine in the presence of acetic acid to give

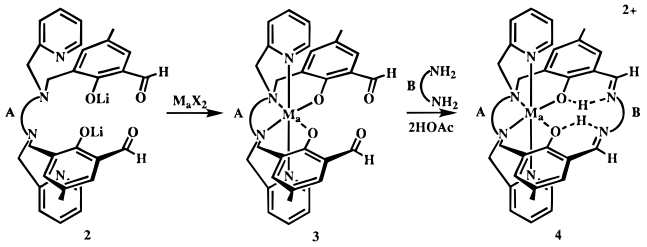

**2** **3** **4**

the protonated monometallic macrocyclic complexes **4**, which also were isolated. These monometallic complexes **4** provide convenient starting materials for the mild introduction of the second metal into the open-site. A variety of diamines were used for linking the macrocycle, but for the present purposes we only refer to combinations of ethylenediamine (en) and trimethylenediamine (tn) links. The nomenclature used to describe the ligand is to designate the closed-site link, A, first followed by the open-site link, B, followed by im to designate the diimine. Thus the four link permutations of the complex **4** are designated as $[M_a(enenim)(H^+)_2]^{2+}$, $[M_a(entnim)(H^+)_2]^{2+}$, $[M_a(tnenim)(H^+)_2]^{2+}$, and $[M_a(tntnim)(H^+)_2]^{2+}$, where the closed-site metal is written first followed by the ligand followed by the occupancy of the open-site. All monometallic complexes of the type **4** have the shown $C_2$ symmetric structure. When a second metal is incorporated, however, the tnenim and tntnim bimetallic complexes remain $C_2$ symmetric with trans-disposed pyridines (see **4**), but those containing an en A-link, entnim and enenim, generally give unsymmetrical complexes in which the two pyridines of the closed-site are cis-disposed. Monometallic cobalt(II) complexes of the type $[Co(enenim)(H^+)_2]^{2+}$ and $[Co(entnim)(H^+)_2]^{2+}$ are oxidized by ferrocinium ($fc^+$) ions to form stable cobalt(III) monometallic complexes. This is not the case for the complexes $[Co(tnenim)(H^+)_2]^{2+}$ and $[Co(tntnim)(H^+)_2]^{2+}$. Acyclic cobalt(II) complexes of the type **3**, however, are readily oxidized by $fc^+$, regardless of whether a trimethylene or dimethylene A-link is present. Because the cobalt(II) to cobalt(III) transformation involves metal−ligand bond contraction, we supposed that the instability of the cobalt(III) complexes of the monometallic tnenim and tntnim complexes arose from the expanded A-link and from the inability of the macrocyclic ligand to adjust to the contracted bond lengths of the cobalt(III) state in the closed-site. In particular, we suspected that the imine groups restricted the flexibility of the macrocyclic system. Thus we wished to explore the effect on the redox potentials when the imine groups were reduced to amines. Connected with this issue was the observation that the dicobalt(II) complexes [Co(entnim)CoCl]$PF_6$ and [Co(tntnim)CoCl]$PF_6$ were inert to $O_2$. We speculated that the corresponding amine ligands incorporating two cobalt(II) atoms might absorb $O_2$ because of the greater flexibility of the amine ligands and their higher base strengths. Finally, the extra flexibility of the amine ligands might cause a change in the stereochemistry of bimetallic complexes compared to those where the imine groups are present. This paper addresses these questions as well as those related to cooperative bimetallic oxidation.

## 1. Preparation of Amine Complexes

We have developed a general and efficient method of preparing the amine complexes from the monometallic imine complexes. This is illustrated in **5** → **6**.

(4) Fraser, C.; Johnston, L.; Rheingold, A. L.; Haggerty, B. S.; Williams, G. K.; Whelan, J.; Bosnich, B. *Inorg. Chem.* **1992**, *31*, 1835−44.
(5) Fraser, C.; Ostrander, R.; Rheingold, A. L.; White, C.; Bosnich, B. *Inorg. Chem.* **1994**, *33*, 324−37.
(6) Fraser, C.; Bosnich, B. *Inorg. Chem.* **1994**, *33*, 338−44.
(7) McCollum, D. G.; Hall, L.; White, C.; Ostrander, R.; Rheingold, A. L.; Whelan, J.; Bosnich, B. *Inorg. Chem.* **1994**, *33*, 924−33.
(8) McCollum, D. G.; Fraser, C.; Ostrander, R.; Rheingold, A. L.; Bosnich, B. *Inorg. Chem.* **1994**, *33*, 2383−92.

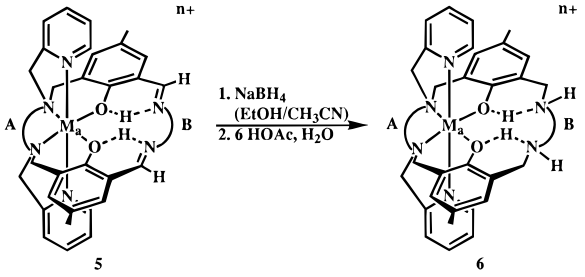


5 6

The reduction of the imine groups is carried out by the slow addition of 1 equiv of $NaBH_4$ in ethanol to a solution of **5** in acetonitrile at 5 °C. Because of the presence of protons in the open-site cavity, reduction of the imine groups by $BH_4^-$ ions is extremely fast. Thus only 1 equiv of $NaBH_4$ is required for complete reduction and no reduction of the metal is observed even when the closed-site metal is cobalt(III). The direct product of the $BH_4^-$ ion reduction is a species which probably encapsulates boron in the open-site, possibly by the formation of amide−boron bonds.[9] Addition of aqueous acetic acid cleaves these bonds to give the open-site protonated amine product **6**. Yields are from 60 to 80%. Attempts to reduce the imines by Pd/C under $H_2$ in methanol[10] were successful in some cases but were limited by the poor solubility of the starting complexes in methanol and by the tendency of the catalytic hydrogenation to get "stuck" requiring, as a consequence, large catalytic loadings. The $BH_4^-$ ion reduction appears to be general and efficient.

The $BH_4^-$ ion reduction method provided the eight following monometallic complexes: $[M(macrocyclicamine)(H^+)_2](PF_6)_2$ where macrocyclicamine[11] = tntnam, tnenam, entnam, and enenam and M = Zn(II) and Co(II). In addition, the four complexes $[Mn(tntnam)(H^+)_2](PF_6)_2$, $[Mn(entnam)(H^+)_2](PF_6)_2$, $[Co(entnam)(H^+)_2](PF_6)_3$, and $[Co(enenam)(H^+)_2](PF_6)_3$ were prepared. The last two were derived by direct $BH_4^-$ ion reduction of the corresponding cobalt(III) imine complexes. The cobalt(II) and manganese(II) complexes are $O_2$ sensitive in acetonitrile solutions but appear to be stable to dioxygen in the solid state. We have not observed a striking qualitative difference between the amine and imine monometallic complexes in their $O_2$ reactivity. All of the amine monometallic complexes have conductivities in acetonitrile solutions consistent with their formulation, the divalent metals are 2:1 electrolytes and the cobalt(III) complexes are 3:1 electrolytes. The $^1H$ NMR spectra in acetonitrile solutions of the diamagnetic zinc(II) and cobalt(III) complexes are consistent with the symmetrical topology **6** and, further, proton integration indicates the presence of four amine protons as would be expected for the diprotonated complex, **6**. Upon the addition of $D_2O$ to the acetonitrile solutions these amine proton signals disappear in the $^1H$ NMR spectra, as expected. The electronic absorption spectra of the amine complexes are very similar to those of the corresponding imine monometallic complexes except that the amine complexes are devoid of the imine ($\pi \rightarrow \pi^*$) transition at ~400 nm.[4−8]

As noted previously, the monometallic cobalt(II) imine complexes $[Co(enenim)(H^+)_2]^{2+}$ and $[Co(entnim)(H^+)_2]^{2+}$ are readily oxidized to their stable cobalt(III) analogues by $fc^+$. This is not the case for the $[Co(tntnim)(H^+)_2]^{2+}$ and $[Co(tnenim)(H^+)_2]^{2+}$ complexes where it was assumed that the presence of the expanded trimethylenediamine closed-site link combined with the rigidity of the imine groups prevented these ligands from assuming the shorter cobalt(III) bond lengths without strain. If this is so, then we would expect that the more flexible monometallic amine complexes, $[Co(tnenam)(H^+)_2]^{2+}$ and $[Co(tntnam)(H^+)_2]^{2+}$, should form stable cobalt(III) complexes. This is indeed the case. We find that all of the cobalt(II) complexes of the amine ligands enenam, entnam, tnenam and tntnam form stable cobalt(III) complexes which were isolated and characterized.

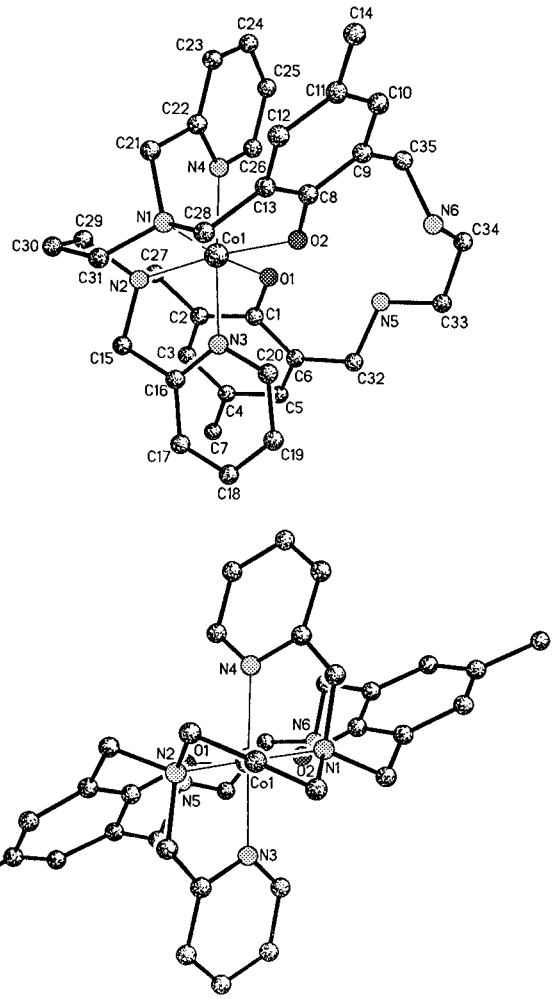


**Figure 1.** Two views of the molecular structure of $[Co(tnenam)(H^+)_2]^{3+}$ (**I**).

The crystal structure of $[Co(tnenam)(H^+)_2](PF_6)_3 \cdot CH_3CN$ is shown in Figure 1. Two perspectives are illustrated, one serves to depict the conformation of the ligand and the other shows the open-site cavity. Hydrogen atom positions were not resolved. The overall topology is as expected with trans disposed pyridine ligands oriented perpendicular to the mean macrocyclic plane. The conformation of the closed-site tn link is skew rather than chair as required for the trans disposition of the pyridine ligands. The rest of the ligand displays considerable conformational twisting. Selected metal−ligand bond lengths and bond angles are listed in Table 2, and Table 1 lists the crystallographic parameters. The dimensions of the open-site cavity are also included in Table 2 where it will be noted that the diagonal dimensions (O(1)−N(6) and O(2)−N(5)) of the pseudosquare represented by O(1)−O(2)−N(6)−N(5) are 4.146 and 3.695 Å, respectively. These dimensions indicate that minor adjustments of the open-site cavity are required to accommodate a first-row transition metal ion.

(9) (a) Mandal, S. K.; Thompson, L. K.; Nag, K.; Charland, J.-P.; Gabe, E. J. *Inorg. Chem.* **1987**, *26*, 1391−95. (b) Grannas, M. J.; Hoskins, B. F.; Robson, R. *Inorg. Chem.* **1994**, *33*, 1071−79.

(10) Beretka, J.; West, B. O.; O'Connor, M. J. *Aust. J. Chem.* **1964**, *17*, 192−201.

(11) In an obvious extension of the nomenclature, the amine ligands are designated by replacing "im" with "am" after the abbreviations for the chelate links. For example, enenim becomes enenam.

**Table 1.** Crystallographic Data for $[Co(tnenam)(H^+)_2](PF_6)_3 \cdot CH_3CN$

| | |
|---|---|
| formula | $C_{37}H_{47}CoF_{18}N_7O_2P_3$ |
| formula weight | 1115.6 |
| crystal system | monoclinic |
| space group | $P2_1/c$ |
| *a*, *b*, *c*, Å | 8.502(3), 24.385(7), 21.976(6) |
| $\beta$, deg | 93.79(3) |
| volume, Å$^3$ | 4546(3) |
| Z | 4 |
| $D_x$, g cm$^{-3}$ | 1.630 |
| $\mu$(Mo K$\alpha$), cm$^{-1}$ | 6.00 |
| *T*, K | 296 |
| diffractometer | Siemens P4 (graphite monochromator) |
| 2$\theta$ range, deg | 4−45 ($\pm h$, $+k$, $+l$ ) |
| rflns (collctd, indpdnt, obsd) | 6082, 5904, 3460 ($4\sigma F_o$) |
| *R(F)*, *R(wF)*,[a] % | 6.68, 7.40 |
| GOF | 1.39 |
| $N_o/N_v$ | 8.1 |

[a] $R(F) = \Sigma\Delta/\Sigma(F_o)$; $R(wF) = \Sigma[\Delta w^{1/2}]/[F_o w^{1/2}]$; $\Delta = |F_o - F_c|$; $w^{-1} = \sigma^2(F_o) + gF_o^2$.

**Table 2.** Selected Bond Distances and Angles for $[Co(tnenam)(H^+)_2](PF_6)_3 \cdot CH_3CN$

| Bond Distances and Cavity Dimensions (Å) | | | |
|---|---|---|---|
| Co(1)−O(1) | 1.924(5) | Co(1)−O(2) | 1.930(5) |
| Co(1)−N(1) | 2.025(6) | Co(1)−N(2) | 2.026(6) |
| Co(1)−N(3) | 1.945(7) | Co(1)−N(4) | 1.964(7) |
| O(1)−C(1) | 1.332(9) | O(2)−C(8) | 1.342(9) |
| O(1)−O(2) | 2.487(11) | N(6)−N(5) | 3.196(11) |
| O(1)−N(5) | 2.658(11) | O(1)−N(6) | 4.146(11) |
| O(2)−N(6) | 2.886(11) | O(2)−N(5) | 3.695(11) |

| Bond Angles (deg) | | | |
|---|---|---|---|
| O(1)−Co(1)−O(2) | 80.4(2) | O(1)−Co(1)−N(1) | 172.8(2) |
| O(2)−Co(1)−N(1) | 93.4(2) | O(1)−Co(1)−N(2) | 93.0(2) |
| O(2)−Co(1)−N(2) | 172.4(2) | N(1)−Co(1)−N(2) | 93.4(3) |
| O(1)−Co(1)−N(3) | 86.7(2) | O(2)−Co(1)−N(3) | 91.8(2) |
| N(1)−Co(1)−N(3) | 97.2(3) | N(2)−Co(1)−N(3) | 84.1(3) |
| O(1)−Co(1)−N(4) | 92.4(2) | O(2)−Co(1)−N(4) | 85.0(2) |
| N(1)−Co(1)−N(4) | 83.4(3) | N(2)−Co(1)−N(4) | 99.0(3) |
| N(3)−Co(1)−N(4) | 176.8(3) | Co(1)−O(1)−C(1) | 123.5(5) |
| | | Co(1)−O(2)−C(8) | 122.7(4) |

## 2. Bimetallic Complexes

These monometallic complexes provide ideal precursors for the introduction of a second metal into the open-site under mild conditions. This general method follows the procedure **6** → **7**

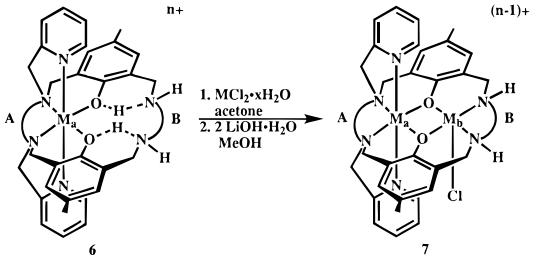


**6** **7**

and is analogous to the methods developed for the imine complexes except that LiOH was required to drive the reaction to completion, whereas $Et_3N$ was sufficient to induce the formation of bimetallic complexes of the less basic imine analogues. For the present purposes we have concentrated on the synthesis of homobimetallic complexes. We shall report on the synthesis of site-specific heterobimetallic complexes later. Generally, these homobimetallic complexes proved to be more soluble and more difficult to crystallize that their imine analogues. The homobimetallic complexes [Zn(enenam)ZnCl]$PF_6$, [Zn(entnam)ZnCl]$PF_6$, [Zn(tnenam)ZnCl]$PF_6$, and [Zn(tntnam)ZnCl]$PF_6$ were prepared. Analogous dicobalt(II) complexes were also prepared with all ligands except for enenam. All of the homobimetallic complexes were fully characterized except for [Co(entnam)CoCl]$PF_6$ and [Co(tntnam)CoCl]$PF_6$. We were unable to obtain satisfactory crystals of these two complexes because of their extreme $O_2$ sensitivity and their solubility properties. They were obtained as powders which displayed electronic spectra which were fully consistent with the bimetallic formulation when compared with the spectrum for the [Co(tnenam)CoCl]$PF_6$ complex. In addition, the three complexes [$Co^{III}$(entnam)$Co^{II}$Cl]$(PF_6)_2$, [$Co^{III}$(tnenam)$Co^{II}$Cl]$(PF_6)_2$, and [$Co^{III}$(tntnam)$Co^{II}$Cl]$(PF_6)_2$ were prepared from the appropriate [$Co^{III}$(macrocyclicamine)$(H^+)_2$]$(PF_6)_3$ starting materials. All of the dicobalt(II) complexes are very $O_2$ sensitive in acetonitrile or methylene chloride solutions. The solids are only slightly less sensitive. This contrasts with the analogous dicobalt(II) complexes of the imine ligands which are stable to dioxygen in solution. It is significant that the [$Co^{III}$(macrocyclicamine)$Co^{II}$Cl]$(PF_6)_2$ complexes do not react with dioxygen in acetonitrile solutions even after prolonged exposure. We discuss the phenomenon later.

The bimetallic complexes of these binucleating macrocyclic amine ligands potentially present extra stereochemical complexity over their imine analogues. This complexity arises from the chirality of the nitrogen atoms in the open-site coupled with the topology of the closed-site. The complexity can be illustrated by the generic structures **8** and **9** using the diamagnetic dizinc(II) complexes as examples. Considering a single

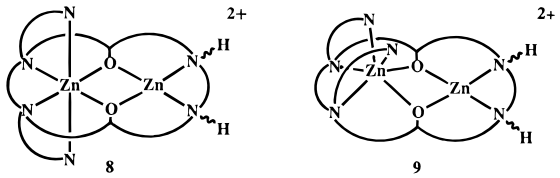


**8** **9**

topological (chiral) isomer for the closed-site of **8**, the open-site nitrogen groups can be (*S*,*S*) or (*R*,*R*) or (*R*,*S*). The first two will be $C_2$ symmetric and the last is $C_1$. Thus the isomers can be designated as *trans*-py-(*R*,*R*) etc. Structure **9** contains *cis*-pyridine groups in the closed-site and the nitrogen groups can be (*S*,*S*) or equivalently (*R*,*R*), and (*R*,*S*). The (*R*,*S*) configuration allows for additional isomers according to whether the open-site link is tilted cis or trans to the cis-pyridine groups of the closed-site. The *cis*-py-(*S*,*S*) or -(*R*,*R*) isomer has $C_1$ symmetry whereas both of the *cis*-py-(*R*,*S*) isomers will have average $C_s$ symmetry provided there is rapid conformational interconversion when 5-membered chelate A and B links are present. When the open-site zinc atom contains a chloro group, additional isomers are possible according to whether the chloro group is cis or trans to the *cis*-pyridine groups for the (*S*,*S*) or (*R*,*R*) isomers. This "up-down" chloro ligand isomerism is also present in either **8** or **9** when the nitrogen group configuration is (*R*,*S*).

The $^1$H NMR spectra of the four dizinc(II) complexes of the type [Zn(macrocyclicamine)ZnCl]$PF_6$ were obtained in acetone-$d_6$ solutions at 25 °C. The complexes were dechlorinated by the addition of 1 equiv of $AgPF_6$ and the $^1$H NMR spectra were monitored. The N−H protons were broad and generally overlapped with other resonances and were not useful for identifying isomers. In nearly all cases the α-pyridyl and *p*-tolylmethyl proton signals were sharp and their chemical shifts were sufficient to identify isomers. The integrated intensities of the two sets of protons were consistent and established the isomer ratios. In most cases the isomer ratios of the chlorinated Zn−ZnCl complexes immediately after dissolution of the solids are not the same as those which are established over 24 h in

**Table 3.** Equilibrium Isomer Distribution[a] of [Zn(macrocyclicamine)ZnCl]$PF_6$ and [Zn(macrocyclicamine)Zn]-$(PF_6)_2$ Complexes in acetone-$d_6$ Solutions at 25 °C

| complex | *trans*-py-(*S*,*S*) | *trans*-py-(*R*,*S*) | *trans*-py-(*R*,*R*) |
|---|---|---|---|
| $[Zn(tntnam)ZnCl]^+$ | 2 [$C_1$][b] | 90 [$C_1$] | 8 [$C_1$] |
| $[Zn(tntnam)Zn]^{2+}$ | 7 [$C_2$] | 81 [$C_1$] | 12 [$C_2$] |
| $[Zn(tnenam)ZnCl]^+$ | 67 [$C_1$] | 22 [$C_1$] | 11 [$C_1$] |
| $[Zn(tnenam)Zn]^{2+}$ | 25 [$C_2$] | 51 [$C_1$] | 24 [$C_2$] |
| $[Zn(entnam)ZnCl]^+$ | 0 | 100 [$C_1$] | 0 |
| $[Zn(entnam)Zn]^{2+}$ | 10 [$C_2$] | 90 [$C_1$] | 0 |

| complex | *cis*-py-(*R*,*S*) | *cis*-py-(*S*,*S*) or -(*R*,*R*) |
|---|---|---|
| $[Zn(enenam)ZnCl]^+$ | 93 [$C_s$] | 7 [$C_1$] |
| $[Zn(enenam)Zn]^{2+}$ | 90 [$C_s$] | 10 [$C_1$] |

[a] The (*S*,*S*) and (*R*,*R*) isomer assignments are arbitrary. [b] The point group designations are consistent with $^1$H NMR data and refer to proposed structures.

acetone solutions at 25 °C. Similarly, the dechlorinated Zn−Zn complexes arrive at new constant isomer ratios after a similar time although the initial ratios obtained immediately after dechlorination are nearly the same as those of the equilibrated chlorinated Zn−ZnCl analogues. This latter observation has allowed us to correlate the Zn−ZnCl isomers with the corresponding Zn−Zn isomers. We assume that the slow isomer equilibration occurs by N−H proton exchange[12] with the residual water in the acetone solvent.

The isomer ratios for the eight dizinc complexes are listed in Table 3. A number of elements in Table 3 require comment. First, where chloro position isomerism is possible for certain isomers only one isomer is observed presumably because of steric effects. Second, at the present level of analysis $^1$H NMR spectroscopy does not distinguish between the *trans*-py-(*R*,*R*) and *trans*-py-(*S*,*S*) diastereomers and the assignment of isomers is arbitrary but is consistent for the same ligand when the Zn−Zn−Cl and Zn−Zn complexes are compared. Third, assignment of the *cis*- and *trans*-py topology, although consistent with results, is also somewhat arbitrary. Previous work on imine complexes indicates that a closed-site tn link will generate the *trans*-py topology for bimetallic complexes but that a closed-site en link generally, but not always, gives a *cis*-py topology. Hence we assign the *trans*-py topology to complexes containing closed-site tn links. The entnam complexes are also assigned the *trans*-py topology principally because, were the *cis*-py topology to obtain, we would expect to find two isomers for the open-site nitrogen group (*R*,*S*) configuration. Only one is observed. The enenam complexes are assigned the *cis*-py topology because, as we show presently, the crystal structure of the (*R*,*S*) isomer has cis pyridines. The presence of a variety of isomers for all of these ligands suggests, perhaps surprisingly, that the topology of the closed-site is insufficient to fix the conformation of the ligand so that a single configuration at the open-site nitrogen groups exists. Presumably there are a number of energetically similar ligand conformations which can be adopted to accommodate various open-site nitrogen group configurations. The presence of these isomers may explain the difficulty we experienced in crystallizing the dicobalt(II) complexes and may prove to be a general phenomenon with other bimetallic complexes of these ligands.

The single-crystal X-ray diffraction structure of [Zn(enenam)-ZnCl]$PF_6$ was determined. The crystal data are shown in Table 4 and selected bond lengths and bond angles are listed in Table 5. The hydrogen atom positions were not located. Two perspectives of the structure are shown in Figure 2. A number of features of this structure bear noting. First, the pyridine groups are cis-disposed as is usually found for imine complexes bearing an en closed-site link. An explanation for this occurrence has been offered previously.[4−8] Second, both sets of amine groups, N(3)/N(4) and N(1)/N(2), are in the meso (*R*,*S*) configuration. To obtain a *cis*-pyridine topology the N(3)/N(4) amine groups are required to adopt the (*R*,*S*) configuration. Third, both of the zinc atoms lie out of the mean macrocyclic plane and there are two crystallographically different molecules in the unit cell (Mol. A and Mol. B) whose geometric parameters are slightly different. The Zn(2) atom lies above the approximate N(3), N(4), O(1), O(2) plane by 0.856 Å (Mol. A) and 0.840 Å (Mol. B) and Zn(1) lies out of the N(1), N(2), O(2), O(1) plane by 0.693 Å (Mol. A) and 0.690 Å (Mol. B) in the opposite direction. Most of the bond length and bond angle data are unexceptional except that both zinc coordination geometries are distorted from the usual 6- and 5-coordinate geometries.

**Table 4.** Crystallographic Data for [Zn(enenam)ZnCl]$PF_6$

| | |
|---|---|
| formula | $C_{34}H_{40}ClF_6N_6O_2PZn_2$ |
| formula weight | 875.9 |
| crystal system | monoclinic |
| space group | $P2_1/c$ |
| *a*, *b*, *c*, Å | 18.957(8), 20.490(10), 21.355(5) |
| $\beta$, deg | 116.25(2) |
| volume, Å$^3$ | 7440(7) |
| Z | 8 |
| $D_x$, g cm$^{-3}$ | 1.564 |
| $\mu$(Mo K$\alpha$), cm$^{-1}$ | 14.8 |
| *T*, K | 296 |
| diffractometer | Siemens P4 (graphite monochromator) |
| $2\theta$ range, deg | 4−45 ($+h$, $+k$, $\pm l$) |
| rflns (collctd, indpdnt, obsd) | 14506, 12021, 9762 ($2\sigma$I) |
| *R(F)*, *R(wF$^2$)*,[a] % | 6.80, 14.65 |
| GOF | 0.96 |
| $N_o/N_v$ | 9.1 |

[a] $R(F) = \Sigma\Delta/\Sigma(F_o)$; $R(wF^2) = [\Sigma[w(F_o^2 - F_c^2)^2]/\Sigma\,[w(F_o^2)^2]]^{1/2}$; $\Delta = |F_o - F_c|$; $w^{-1} = \sigma^2(F_o) + gF_o^2$.

**Table 5.** Selected Bond Distances and Angles for [Zn(enenam)ZnCl]$PF_6$

| | | | |
|---|---|---|---|
| Bond Distances (Å) | | | |
| Zn(1)−Zn(2) | 3.276(2) | Zn(2)−O(1) | 2.012(5) |
| Zn(1)−Cl | 2.270(3) | Zn(2)−O(2) | 2.139(5) |
| Zn(1)−O(1) | 1.989(5) | Zn(2)−N(3) | 2.228(7) |
| Zn(1)−O(2) | 2.061(5) | Zn(2)−N(4) | 2.206(7) |
| Zn(1)−N(1) | 2.177(7) | Zn(2)−N(5) | 2.171(7) |
| Zn(1)−N(2) | 2.102(7) | Zn(2)−N(6) | 2.183(8) |
| O(1)−C(6) | 1.340(9) | O(2)−C(13) | 1.320(9) |
| Bond Angles (deg) | | | |
| O(1)−Zn(1)−O(2) | 74.9(2) | O(1)−Zn(2)−O(2) | 72.7(2) |
| O(1)−Zn(1)−N(1) | 84.2(2) | O(1)−Zn(2)−N(3) | 150.2(3) |
| O(1)−Zn(1)−N(2) | 137.2(3) | O(1)−Zn(2)−N(4) | 89.0(2) |
| O(1)−Zn(1)−Cl | 114.5(2) | O(1)−Zn(2)−N(5) | 88.7(2) |
| O(2)−Zn(1)−N(1) | 143.7(3) | O(1)−Zn(2)−N(6) | 118.5(3) |
| O(2)−Zn(1)−N(2) | 90.2(2) | O(2)−Zn(2)−N(3) | 85.1(2) |
| O(2)−Zn(1)−Cl | 108.7(2) | O(2)−Zn(2)−N(4) | 113.8(2) |
| N(1)−Zn(1)−N(2) | 85.3(3) | O(2)−Zn(2)−N(5) | 156.7(3) |
| N(1)−Zn(1)−Cl | 106.9(2) | O(2)−Zn(2)−N(6) | 86.1(2) |
| N(2)−Zn(1)−Cl | 108.2(2) | N(3)−Zn(2)−N(4) | 82.1(3) |
| Zn(1)−O(1)−Zn(2) | 109.9(2) | N(3)−Zn(2)−N(5) | 117.0(3) |
| C(6)−O(1)−Zn(1) | 115.0(5) | N(3)−Zn(2)−N(6) | 78.2(3) |
| C(6)−O(1)−Zn(2) | 127.5(5) | N(4)−Zn(2)−N(5) | 78.8(3) |
| Zn(1)−O(2)−Zn(2) | 102.5(2) | N(4)−Zn(2)−N(6) | 150.6(3) |
| C(13)−O(2)−Zn(1) | 128.5(5) | N(5)−Zn(2)−N(6) | 90.9(3) |
| C(13)−O(2)−Zn(2) | 121.4(5) | | |

## 3. Electrochemistry and Oxidative Reactivity

In order for these binucleating macrocyclic ligand complexes to act as 2-metal redox systems the required oxidation states of

(12) Halpern, B.; Sargeson, A. M.; Turnbull, K. R. *J. Am. Chem. Soc.* **1966**, *88*, 4630−36.

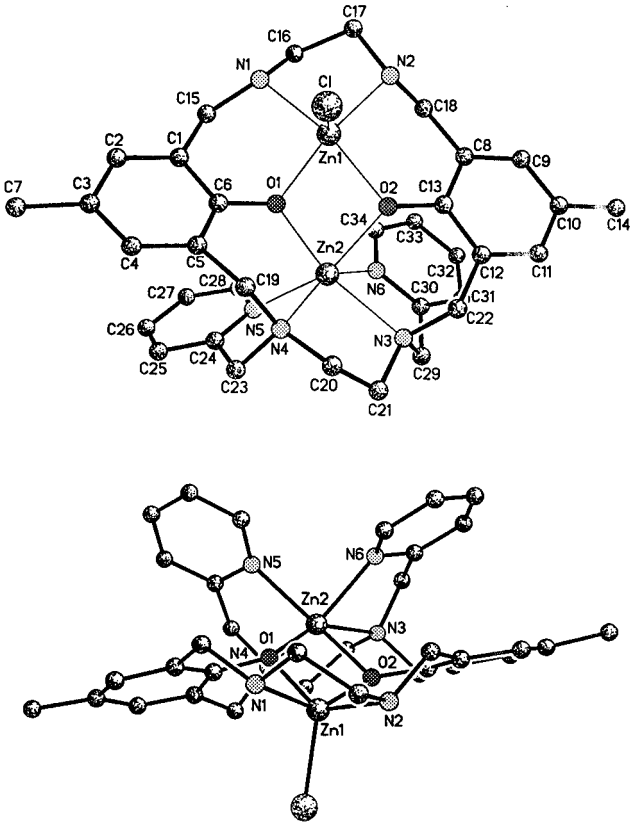


**Figure 2.** Two views of the molecular structure of one of the two independent molecules of $[Zn(enenam)ZnCl]^+$ (**II**) showing the placements of the Zn atoms.

**Table 6.** Redox Potentials for the M(II)/M(III) Couples of Complexes Derived from the Macrocyclicimine and Macrocyclicamine Binucleating Ligands[a,b]

| complex | $E_f$ (V) | $E_{pa} - E_{pc}$ (V) |
|---|---|---|
| $[Co(enenim)ZnCl]^{2+}$ | −0.37 | 0.105 |
| $[Co(entnim)ZnCl]^{2+}$ | −0.37 | 0.155 |
| $[Co(tnenim)ZnCl]^{+}$ | −0.10 | 0.070 |
| $[Co(tntnim)ZnCl]^{+}$ | −0.11 | 0.069 |
| $[Mn(tntnim)(H^+)_2]^{2+}$ | 0.40 | 0.102 |
| $[Mn(entnim)(H^+)_2]^{2+}$ | 0.21 | 0.073 |
| $[Mn(tntnam)(H^+)_2]^{2+}$ [c] | −0.01 | 0.073 |
| $[Mn(entnam)(H^+)_2]^{2+}$ | −0.08 | 0.084 |
| $[Fe(tntnim)(H^+)_2]^{2+}$ | −0.01 | 0.059 |
| $[Fe(entnim)(H^+)_2]^{2+}$ | −0.15 | 0.066 |

[a] Conditions: $5 \times 10^{-4}$ M complex and 0.1 M *n*-$Bu_4NPF_6$ in $CH_3CN$; Pt button working electrode; Pt wire auxiliary electrode; $Ag/AgNO_3$ reference electrode. [b] Potentials are referenced to the $fc/fc^+$ internal standard set to zero. (c) A second wave was observed at 0.77 V versus $fc/fc^+$ ($E_{pa} - E_{pc} = 0.096$ V).

both metals must be accessible for a particular oxidant. The relevant oxidation states were explored for a number of systems by cyclic voltammetry and by employing the ferrocinium ion for oxidation where irreversible waves were observed. In this and the succeeding section we address the following issues. First, we investigate the relationship between closed-site Co(II)/Co(III) potentials and the closed-site and open-site links in both imine and amine complexes. Second, we determine whether the redox behavior observed for the Co(II)/Co(III) couples also applies to Mn(II)/Mn(III) and Fe(II)/Fe(III) potentials for both the imine and some amine complexes. Third, we explore the effect on the Co(II)/Co(III) potentials when the other metal is oxidized in bimetallic complexes.

A series of redox potentials are listed in Table 6 and are quoted relative to the $fc/fc^+$ potential.[13] The first four bimetallic Co(II)/Co(III) potentials were reported previously[4−8] and they serve to illustrate that the open-site link is unimportant in controlling the potentials but that the closed-site link can have a strong influence on the potentials. The increase in redox potentials that is observed when the closed-site en link is replaced by tn in these bimetallic complexes also obtains for the analogous four monometallic complexes, $[Co(macrocyclicimine)(H^+)_2]^{2+}$, for which ferrocinium ions only oxidize the systems with an en closed-site link. It thus appears that ligand structural factors can affect the redox potentials. Specifically, we ascribed these variations to the presence of the larger chelate bite tn link at the closed-site being restrained by the rigid imine groups from adjusting to the shorter bond lengths of cobalt(III). Consistent with this hypothesis is our observation that ferrocinium ions oxidize all four of the amine monometallic cobalt(II) complexes, $[Co(enenam)(H^+)_2]^{2+}$, $[Co(entnam)(H^+)_2]^{2+}$, $[Co(tnenam)(H^+)_2]^{2+}$, and $[Co(tntnam)(H^+)_2]^{2+}$, to stable cobalt(III) complexes. We were unable to obtain suitable reversible waves with these four complexes to report reliable Co(II)/Co(III) potentials. This effect on the redox potentials by conformational restraints is referred to as mechanical coupling in analogy to the concept of molecular mechanics strain energy. As in the case of molecular mechanics, molecular coupling refers to the energy terms associated with bond stretches, bond angle bends, torsional deformations, van der Waals, and electrostatic interactions.

It could be argued that this mechanical coupling is evident in these Co(II)/Co(III) potentials because the cobalt(III) state demands that its 6-coordinate complexes be octahedral whereas other metals, less restrictive in their geometric demands, may not show pronounced mechanical coupling. This supposition does not appear to be the case as is shown in Table 6 where the manganese(II) and iron(II) imine complexes show that the complexes containing closed-site tn links display more positive potentials than do the analogous complexes with en links. Further, the analogous amine complexes of the manganese(II) complexes show more negative potentials compared to their imine counterparts. In the context of the mechanical coupling model it is interesting to note that the difference between the redox potentials of the entnim and tntnim complexes is 0.26 V for Co(II)/Co(III), 0.19 V for Mn(II)/Mn(III), and 0.14 V for Fe(II)/Fe(III) potentials. This decrease in the differences in the order, Co > Mn > Fe, probably follows the structural demands of the higher oxidation states of the metal and gives some credence to the assertion that a metal with more rigid stereochemical demands in the higher oxidation state will have greater mechanical coupling for these ligands. Differences in redox potentials, however, reflect the energies of both the lower and higher oxidation states and it is not certain which of these has a greater effect in controlling the redox differences.

A different source of mechanical coupling appears to control the redox potentials in homobimetallic cobalt complexes. This is revealed by the oxidation of the dicobalt(II) complexes with ferrocinium ions (eq 1), where macrocyclicamine = tntnam,

$$[Co^{II}(\text{macrocyclicamine})Co^{II}Cl]PF_6 \xrightarrow{2[Cp_2Fe]PF_6} [Co^{III}(\text{macrocyclicamine})Co^{II}Cl](PF_6)_2 \quad (1)$$

tnenam, entnam. The use of 2 equiv of $fc^+$ in acetonitrile solution led only to the oxidation of the closed-site cobalt ion; 1 equiv of $fc^+$ remained. That oxidation of the closed-site cobalt ion had occurred was established by a number of methods. First, the presence of cobalt(III) is established by the appearance of

(13) Gagné, R. R.; Koval, C. A.; Lisensky, G. C. *Inorg. Chem.* **1980**, *19*, 2854−55.

moderately strong ($\epsilon \sim 2000$) phenolate−cobalt(III) charge transfer bands in the 420−440-nm region and by broad d−d transitions in the 560−600-nm region. Second, whereas the dicobalt(II) complexes have very weak ($\epsilon \sim 20$) d−d transitions encompassing the 400−1100-nm region, the closed-site cobalt(II) has a characteristic transition in the 960−1000-nm region while the open-site cobalt(II) displays absorption centered at 1040−1100 nm.[14] All of the products of $fc^+$ oxidation (eq 1) displayed phenolate−cobalt(III) charge transfer bands, d−d transitions, and an absorption at 1040−1100 nm. The closed-site Co(III)−open-site Co(II) assignments were supported by the reactions depicted in eqs 2 and 3. Addition of LiOH

$$[Co^{III}(\text{macrocyclicamine})(H^+)_2](PF_6)_3 \xrightarrow[\text{MeOH, acetone}]{\text{(i) LiOH·H}_2\text{O; (ii) CoCl}_2\cdot 6\text{H}_2\text{O}} [Co^{III}(\text{macrocyclicamine})Co^{II}Cl](PF_6)_2 \quad (2)$$

$$[Co^{III}(\text{macrocyclicamine})Co^{II}Cl](PF_6)_2 \xrightarrow[\Delta]{NH_4PF_6,\ H_2O} [Co^{III}(\text{macrocyclicamine})(H^+)_2](PF_6)_3 \quad (3)$$

followed by $CoCl_2$ to the independently prepared monometallic cobalt(III) complexes gave the mixed oxidation state products (eq 2) which were identical to the species prepared by $fc^+$ oxidation (eq 1). Further, heating the mixed oxidation products in water gave the monometallic cobalt(III) complexes (eq 3). It thus appears that after the closed-site cobalt ion is oxidized, the open-site cobalt(II) is not oxidized by $fc^+$ ions. This was confirmed by the fact that $fc^+$ ions did not oxidize the open-site cobalt(II) in the independently prepared mixed oxidation state complexes. These observations suggest, but do not establish, that cobalt(III) is more stable in the closed-site but the results do not establish whether stable open-site cobalt(III) complexes can be prepared. We address these questions next where we investigate the reactivity of $NO^+$ ions and $O_2$ with these complexes. Addition of $NO^+$ ions to the dicobalt(II) complexes of tntnam, tnenam, or entnam could lead to two types of products. First, the $NO^+$ ions could add to the open-site cobalt(II) and induce two-electron transfer from both cobalt(II) ions to produce dicobalt(III)−$NO^-$ complexes (eq 4). Such a

$$[Co^{II}(\text{macrocyclicamine})Co^{II}Cl]PF_6 \xrightarrow{NOPF_6} [Co^{III}(\text{macrocyclicamine})Co^{III}(NO)Cl](PF_6)_2 \quad (4)$$

reaction would fulfill one of our initial objectives. The second mode of reaction with $NO^+$ ions would simply involve electron transfer and lead to the oxidation of one or both of the cobalt(II) ions without nitrosyl addition. Addition of 1 equiv of $NOPF_6$ to alkylnitrile solutions of the $[Co(tntnam)CoCl]PF_6$ and $[Co(entnam)CoCl]PF_6$ complexes led to the formation of the mixed oxidation state complexes $[Co^{III}(tntnam)Co^{II}Cl]^{2+}$ and $[Co^{III}(entnam)Co^{II}Cl]^{2+}$, respectively. As previously described for the $fc^+$ ion oxidations (eq 3), heating these mixed oxidation state complexes in water led to the isolation of the closed-site monometallic cobalt(III) complexes. The reaction of $NO^+$ ions with $[Co^{II}(tnenam)Co^{II}Cl]PF_6$ gave a mixed oxidation state product but because of extensive overlap of absorption bands we were unable to identify the site occupancy of the cobalt(III) ion with certainty. The most consistent inference from the electronic absorption data is that both mixed oxidation state complexes are formed, one with the cobalt(III) ion in the closed-site and the other with the cobalt(III) ion in the open-site. Heating this product in water, however, gave the monometallic cobalt(III) ion, $[Co(tnenam)(H^+)_2]^{3+}$. In these three $NO^+$ ion oxidations, the products containing closed-site cobalt(III) could be produced in two ways. Outer-sphere electron transfer beween the $NO^+$ ion and closed-site cobalt(II) would generate these mixed oxidation complexes directly. Alternatively, an inner-sphere mechanism could be invoked in which $NO^+$ first oxidizes the open-site cobalt(II) to cobalt(III), and then electron transfer occurs from the closed-site cobalt(II) to the open-site cobalt(III). We have been unable to find any firm evidence which would discriminate between these two mechanisms. That the open-site cobalt(II) can be oxidized by an inner-sphere electron transfer mechanism for all three dicobalt(II) ligand systems is demonstrated by their reactions with $O_2$.

When either of the complexes $[Co(tntnam)CoCl]PF_6$ or $[Co(tnenam)CoCl]PF_6$ or $[Co(entnam)CoCl]PF_6$ is dissolved in $CH_2Cl_2$, acetone, or acetonitrile solutions at 25 °C and exposed to atmospheric oxygen the solutions rapidly darken. After ∼2 h of exposure the reactions appear to be complete. Visible−near-IR spectra in all cases show the appearance of phenolate−cobalt(III) charge transfer bands and cobalt(III) d−d transitions, and it is clear that metal oxidation occurred. In all cases transitions in the 960−1000-nm region, indicative of closed-site cobalt(II), were observed. Hence the reaction with dioxygen, in contrast to $fc^+$ oxidation, leads to the oxidation of the open-site cobalt ion. Prolonged exposure to dioxygen does not lead to the oxidation of the closed-site cobalt ion. We were unable to isolate any dioxygen adducts and neither were we able to identify their characteristic electronic absorptions with certainty because of the intrusion of other absorptions in the regions where cobalt(III) dioxygen adducts are expected to absorb.[15] It is probable that the oxidation of the open-site cobalt with dioxygen occurs by one-electron oxidative addition of the $O_2$ to this cobalt to form a cobalt(III)−superoxide intermediate which could then couple to the open-site of another dicobalt(II) molecule to produce a dimer of the type $[Co^{II}-Co^{III}-O-O-Co^{III}-Co^{II}]^{2+}$. This is a common observation with monomeric cobalt(II) amine complexes.[16] There are of course other possibilities involving the superoxide intermediate. Although oxidation by dioxygen appears to be complex and the dioxygen adducts appear to be unstable, the assertion that only the open-site cobalt is oxidized in all cases is secure. Thus, addition of acetic acid to an acetonitrile solution of the product of oxidation of $[Co(entnam)CoCl]PF_6$ by dioxygen led to the isolation of the mixed oxidation state complex, $[Co^{II}(entnam)Co^{III}(OAc)(NCCH_3)](PF_6)_2$, which was fully characterized. Similarly, oxidation of $[Co(tnenam)CoCl]PF_6$ by $O_2$ in $CH_2Cl_2$ led to low-yield precipitation of a product possessing all of the spectroscopic characteristics expected of a mixed oxidation state dicobalt system with the cobalt(III) ion in the open-site. These three open-site cobalt(III)−closed-site cobalt(II) complexes are kinetic products which when heated in water are transformed to monometallic complexes of the type $[Co^{III}(\text{macrocyclicamine})(H^+)_2]^{3+}$. Presumably electron transfer is induced to generate cobalt(III) in the favored closed-site. It thus appears that for dicobalt(II) complexes of these three ligands either site can be oxidized but the closed-site is more stable. As noted previously, however, for the $[Co^{III}(\text{macrocyclicamine})Co^{II}Cl]^{2+}$ complexes the open-site is not oxidized by $fc^+$ when cobalt(III) is present in the closed-site. The converse is also true: $fc^+$

(14) The exact positions of these bands are dependent on the ligand system (see the Experimental Section).

(15) (a) Solomon, E. I.; Tuczek, F.; Root, D. E.; Brown, C. A. *Chem. Rev.* **1994**, *94*, 827−56. (b) Lever, A. B. P.; Gray, H. B. *Acc. Chem. Res.* **1978**, *11*, 348−55.

(16) (a) Jones, R. D.; Summerville, D. A.; Basolo, F. *Chem. Rev.* **1979**, *79*, 139−79. (b) Bosnich, B.; Poon, C. K.; Tobe, M. L. *Inorg. Chem.* **1966**, *5*, 1514−17. (c) See ref 15b.

ions do not oxidize the closed-site cobalt(II) in the mixed oxidation state complex $[Co^{II}(entnam)Co^{III}(OAc)(NCCH_3)](PF_6)_2$.

It thus appears that the presence of cobalt(III) in one of the sites inhibits the oxidation of the cobalt(II) in the other site. The reasons for this phenomenon are probably complex and we have considered three factors. First, it is possible that unfavorable charge−charge interactions exist when two contiguous cobalt(III) ions are present so that oxidation of one cobalt deactivates the other toward oxidation. Second, electronic through-bond coupling could occur[17] which, depending on the structure of the system, might lead to deactivation of double oxidation. Third, a form of mechanical coupling connected with the structural stability of cobalt(III) complexes may operate. Thus when one of the cobalt ions is oxidized to cobalt(III) the ligand is forced to adjust to the shorter bond lengths and to the rigidity of the octahedral cobalt(III) topology. This, in turn, will restrict the conformational flexibility of the ligand in the other site so that unfavorable conformational restrictions are placed on the oxidation of the second cobalt. As we noted earlier, different links (A and B) tend to support different topologies about the closed-site cobalt so that in addition to conformational effects the different topologies that may be adopted by different ligands may alter the nature of the mechanical coupling.

## 4. Discussion

Although the ultimate objective of this work, namely the observation of one-metal localized two-metal oxidative addition, has not been realized, the work has been revealing in the factors which may control such events in synthetic and biological systems. The concept of mechanical coupling is clearly illustrated by the observation that monocobalt(II) imine complexes of the tntnim and tnenim are not oxidized by $fc^+$ ions but oxidation occurs when these complexes are reduced to the amines. Mechanical coupling extends to other metals such as manganese(II) and iron(II) although the effect is less pronounced in these structurally less demanding metals. The oxidation of the dicobalt(II) amine complexes with $fc^+$, $NO^+$, and $O_2$ led to the oxidation of one of the cobalt ions, the site occupancy of which depended on the oxidant. The restriction to oxidation of the other metal probably also includes a form of mechanical coupling where the structural rigidity of the oxidized cobalt restricts the ligand conformation about the other metal. A variety of crystal structures of bimetallic complexes of the imine ligands indicate that the open-site metal can adopt a distorted structure where the two oxygen and two nitrogen donor atoms of the open-site are significantly twisted from the square plane.[4−8] This may also be the case for the present amine ligands. If this structure is rigidly maintained after the system undergoes one-electron oxidation, either by the existing constraints of the ligand or by the generation of a kinetically inert metal center, the resultant complex may become stuck in a conformation which prohibits further oxidation. This mechanical coupling due to the oxidation of one of the metals, however, can act in two ways. As is probable in the present cases, oxidation of one metal may lead to a ligand conformation which resists oxidation of the other metal. On the other hand, it is conceivable that with a properly designed binucleating ligand the oxidation of one metal may induce conformational changes which are conducive to the oxidation of the second metal. Such cooperative mechanical coupling is believed to operate in the oxygenation of hemoglobin.[16a]

Although we suspect that mechanical coupling is the major cause in inhibiting two-metal oxidation in the present systems it may not be the only factor. It is possible that unfavorable electrostatic interactions would exist when both contiguous metals are oxidized so that after the first metal is oxidized the oxidation of the second metal is inhibited by the increased residual positive charge on the first metal. Of course in a fully configured molecular mechanics force field these electrostatic interactions would be included in describing the mechanical coupling if a reliable method of calculating the metal charges were known. Another possible form of metal−metal interaction is covalent through-bond coupling.[17] In bridging bimetallics, through-bond coupling could occur by the interactions of the appropriate metal orbitals with those of the bridging atoms as is commonly described for superexchange. The magnitude of this through-bond coupling is likely to be critically dependent on the bridging structure which affects the overlap of the requisite orbitals.[17] Since it is difficult to unambiguously separate mechanical from through-bond coupling, the existence of significant through-bond coupling in bimetallic oxidations remains an unresolved question.

There are, however, a number of bimetallic systems[18] which exhibit similar behavior where strong mechanical coupling may be absent. Two such examples are illustrated in **10**[19] and **11**.[20]

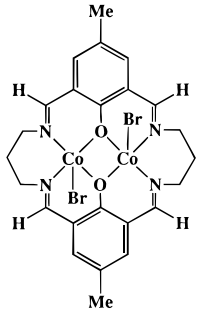


**10**

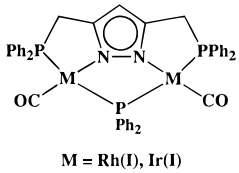


M = Rh(I), Ir(I)

**11**

Addition of an excess of $Br_2$ to **10** led to the initial formation of a dicobalt(III) complex which spontaneously transformed to the mixed oxidation state cobalt(II)−cobalt(III) complex by release of $Br_2$. X-ray diffraction studies of the reduced and mixed oxidation state complexes revealed very small structural differences in the ligand structure and coordinates of the cobalt ions. Similarly, a variety of oxidative-addition reactions involving the homobimetallic complexes **11** clearly demonstrate that after oxidative-addition occurs at one of the metals, the other metal becomes deactivated to oxidative-addition. Systems **10** and **11** appear to be sufficiently rigid to preclude large conformational mechanical coupling. In these two cases, **10**

(17) (a) Hoffmann, R. *Acc. Chem. Res.* **1971**, *4*, 1−9. (b) Kahn, O.; Charlot, M. F. *Nouv. J. de Chem.* **1980**, *4*, 567−76. (c) Gillon, B.; Cavata, C.; Schweiss, P.; Journaux, Y.; Kahn, O.; Schneider, D. *J. Am. Chem. Soc.* **1989**, *111*, 7124−32.

(18) (a) Pessiki, P. J.; Khangulov, S. V.; Ho, D. M.; Dismukes, G. *J. Am. Chem. Soc.* **1994**, *116*, 891−97. (b) Kolel-Veetil, M. K.; Rheingold, A. L.; Ahmed, K. J. *Organometallics* **1993**, *12*, 3439−46. (c) Halpern, J. *Inorg. Chim. Acta* **1982**, *62*, 31−37. (d) Kanda, W.; Nakamura, M.; Okawa, H.; Kida, S. *Bull. Chem. Soc. Jpn.* **1982**, *55*, 471−76. (e) Gagné, R. R.; Spiro, C. L.; Smith, T. J.; Hamann, C. A.; Thies, W. R.; Shiemke, A. K. *J. Am. Chem. Soc.* **1981**, *103*, 4073−81.

(19) (a) Pilkington, N. H.; Robson, R. *Aust. J. Chem.* 1970, *23*, 2225−36. (b) Hoskins, B. F.; Williams, G. A. *Aust. J. Chem.* **1975**, *28*, 2593−605. (c) Hoskins, B. F.; Williams, G. A. *Aust. J. Chem.* **1975**, *28*, 2607−14. (d) Hoskins, B. F.; Robson, R.; Williams, G. A. *Inorg. Chim. Acta* **1976**, *16*, 121−33. (e) Williams, G. A.; Robson, R. *Aust. J. Chem.* **1981**, *34*, 65−79.

(20) (a) Schenck, T. G.; Downes, J. M.; Milne, C. R. C.; Mackenzie, P. B.; Boucher, H.; Whelan, J.; Bosnich, B. *Inorg. Chem.* **1985**, *24*, 2334−37. (b) Schenck, T. G.; Milne, C. R. C.; Sawyer, J. F.; Bosnich, B. *Inorg. Chem.* **1985**, *24*, 2338−44.

and **11**, it is clear that some form of communication exists between metals and it may be that the major interaction is connected with through-space electrostatic coupling and/or through-bond coupling. It is recognized, however, that the metal-ligand bond lengths contract upon oxidation and, as a consequence, the bond lengths of the other metal may change so that mechanical coupling could be introduced. Thus even in rigid bimetallic systems it is difficult to separate the factors governing bimetallic cooperativity. Further, since only a few kcal/mol can cause significant chemical changes, the identification of factors affecting reactivity is made difficult.

The systems **10** and **11** are not strictly analogous to the systems described here. Whereas **10** and **11** involve oxidative addition at both metals, our systems are designed to induce substrate addition at one metal center, while allowing both metals to contribute electrons for substrate reduction. This distinction introduces the issue of barriers to electron transfer since in our cases electron transfer is required to occur from the closed-site metal to the open-site metal bearing the substrate. Given that the rate of electron transfer depends on ligand reorganization, mechanical coupling energies may be crucial in controlling the rates so that even if the reactions were possible thermodynamically their kinetics may prevent reaction. It may therefore be necessary to use stereochemically labile oxidizable metals and flexible ligand systems in order to obtain cooperative two-metal oxidative additions of the type considered here. The results presented here may serve to delineate the factors governing the oxygen uptake in hemerythrin in particular and the cooperative electron transfer activity of multimetallic proteins in general.

## 5. Experimental Section

Conductance measurements were made at 25 °C with a YSI Model 35 conductance meter on 0.001 M $CH_3CN$ solutions of the complexes. Infrared spectra were recorded as Nujol mulls on a Nicolet 20 SXB FTIR spectrometer. The UV/vis solution spectra were obtained on a Varian (Cary) 2400 spectrophotometer using spectral grade $CH_3CN$. Magnetic susceptibilities were measured on powdered samples using a Johnson-Mathey-Evans magnetic susceptibility balance. Cyclic voltammograms were recorded using a Bioanalytical Systems BAS 100 electrochemical analyzer on deaerated $CH_3CN$ solutions which were 0.1 M in *n*-$Bu_4NPF_6$ supporting electrolyte and $5 \times 10^{-4}$ M in sample. Redox couples were measured using a Pt button working electrode, a $Ag/AgNO_3$ non-aqueous reference electrode, and a Pt wire auxiliary electrode and are tabulated versus a ferrocene standard.[13] All samples were dried to constant weight under high vacuum (0.25 mm) prior to analysis. Ethanol refers to absolute ethanol. Acetone was dried over 4 Å molecular sieves. All solvents, $CH_3CH_2CN$, $CH_3CN$, and $CH_2Cl_2$, used in the Reactivity Studies were distilled twice over $CaH_2$. The preparations of the acyclic dialdehyde precursor ligands enal$H_2$[4] and tnal$H_2$[7] have been reported previously. All preparations of Co(II), Mn(II), and Fe(II) complexes were conducted under Ar using deaerated solvents and standard Schlenk techniques. All complexes are air stable as solids unless denoted otherwise.

**Monometallic Complexes. [Li$_2$(dialdehyde)] Complexes.**[21] The dialdehyde complexes were prepared by the general method described for the preparation of the [$Li_2$(tnal)] complex. The electronic spectra of these complexes showed ligand-based absorptions at $\lambda_{max} = 380-390$ nm, $\epsilon = 1.3 \times 10^4$ L mol$^{-1}$cm$^{-1}$, in THF solutions. The complexes are nonelectrolytes in THF.

**[Li$_2$(tnal)].** To the crude tnal$H_2$ (6.07 g, 11.0 mmol) in ethanol (10 mL) was added $Et_3N$ (3.06 mL, 22.0 mmol) and LiCl (0.94 g, 22 mmol) in ethanol (15 mL). A yellow solid precipitated immediately. The mixture was stirred for 1 h. The solid was then collected, washed with ethanol ($2 \times 5$ mL), $Et_2O$ ($2 \times 5$ mL), and pentane ($2 \times 3$ mL), and dried under vacuum. The crude [$Li_2$(tnal)] was obtained as a yellow solid (2.15 g, 3.81 mmol, 35%). The crude salt was recrystallized by dissolving it in THF (~2 mL per gram of complex) and adding $Et_2O$ to induce precipitation (~5 mL per gram). Pure [$Li_2$(tnal)] was obtained as yellow plates. Yield: 20%. The $^1$H NMR spectrum in THF-$d_8$ solution was broad in the aliphatic region ($\delta$ 2.0−5.0) at 25 °C. The spectrum sharpened up as the temperature was lowered. The reported spectrum was recorded at −50 °C. $^1$H NMR (400 MHz, THF-$d_8$, −50 °C): $\delta$ 2.14 (m, 8H); 2.5 (d, $J = 11.7$ Hz, 2H); 2.81 (d, $J = 10.2$ Hz, 2H); 3.18 (d, $J = 15.3$ Hz, 2H); 3.29 (m, 2H); 4.08 (d, $J = 15.2$ Hz, 2H); 4.32 (d, $J = 10.2$ Hz, 2H); 6.43 (d, $J = 7.8$ Hz, 2H); 6.67 (d, $J = 2.0$ Hz, 2H); 6.76 (t, $J = 6.1$ Hz, 2H); 7.01 (d, $J = 2.2$ Hz, 2H); 7.21 (td, $J = 7.6$, 1.6 Hz, 2H); 8.46 (d, $J = 3.4$ Hz, 1H); 9.02 (s, 2H). Anal. Calcd for $C_{33}H_{34}N_4O_4Li_2$: C, 70.20; H, 6.08; N, 9.93; Li, 2.46. Found: C, 70.29; H, 6.03; N, 9.75; Li, 2.33.

**[Li$_2$(enal)].** The pure complex was obtained as yellow plates after recrystallization from THF−$Et_2O$. Yield: 20%. The $^1$H NMR spectrum in THF-$d_8$ solution was broad in the aliphatic region ($\delta$ 2.0−5.0) at 25 °C. The broadness persisted at lower temperatures, although a sharp spectrum was obtained at −100 °C. This spectrum indicated the presence of two components. $^1$H NMR (400 MHz, THF-$d_8$, −100 °C): major isomer, $\delta$ 2.13 (s, 6H); 2.45 (br s, 2H); 3.15 (br d, $J = 12$ Hz, 2H); 3.28 (br m, 2H); 3.54 (br m, 2H); 3.71 (br m, 2H); 3.92 (d, $J = 14$ Hz, 2H); 6.96 (m, 4H); 7.11 (t, $J = 6.0$ Hz, 2H); 7.25 (d, $J = 7.1$ Hz, 2H); 7.57 (t, $J = 7.5$ Hz, 2H); 8.33 (d, $J = 4.1$ Hz, 2H); 9.46 (s, 2H); minor isomer, $\delta$ 2.09 (s, 3H); 2.16 (s, 3H); 2.72 (d, $J = 11$ Hz, 1H); 2.85 (d, $J = 16$ Hz, 1H); 3.79 (t, $J = 14$ Hz, 1H); 4.27 (d, $J = 15$ Hz, 1H); 6.64 (d, $J = 7.6$ Hz, 1H); 6.81 (br s, 1H); 7.05 (br s, 1H); 7.17 (m, 1H); 7.36 (m, 1H); 7.47 (d, $J = 8.0$ Hz, 1H); 7.86 (t, $J = 7.1$ Hz, 1H); 8.44 (d, $J = 3.9$ Hz, 1H); 8.71 (d, $J = 3.5$ Hz, 1H); 9.29 (br s, 1H); 9.60 (br s, 1H). The ratio of the isomers is 90:10 based on the aldehyde resonances. In the spectrum of the major isomer, the appearance of one singlet at 2.13 ppm corresponding to the *p*-tolyl methyl protons and one singlet at 9.46 ppm corresponding to the aldehyde protons confirms the magnetic equivalence of similar protons in this isomer, and is consistent with $C_2$ or $C_s$ symmetry. The minor isomer shows two singlets at 2.09 and 2.16 ppm corresponding to the *p*-tolyl methyl protons, and two singlets at 9.29 and 9.60 ppm corresponding to the aldehyde protons. This result confirms the magnetic inequivalence of similar protons in this isomer, and is consistent with $C_1$ symmetry. Anal. Calcd for $C_{32}H_{32}N_4O_4Li_2$: C, 69.81; H, 5.87; N, 10.18; Li, 2.52. Found: C, 70.08; H, 5.78; N, 10.13; Li, 2.25.

**Monometallic Complexes. [M(diimine)(H$^+$)$_2$](PF$_6$)$_n$ Complexes ($n = 2, 3$).** The preparations of all the monometallic complexes of the diimine ligands containing Zn(II), Co(II), and Co(III) have been reported previously.[8] The same procedures were followed in the preparations of the Mn(II) complexes [Mn(tntnim)(H$^+$)$_2$](PF$_6$)$_2$[22] and [Mn(entnim)(H$^+$)$_2$](PF$_6$)$_2$.

**[Mn(tntnim)(H$^+$)$_2$](PF$_6$)$_2$.** The [Mn(tntnim)(H$^+$)$_2$](PF$_6$)$_2$ (69%) was obtained as red-orange needles after recrystallization from $CH_3CN$−EtOH. $\Lambda_m = 275\ \Omega^{-1}$ mol$^{-1}$ cm$^2$. UV [$\lambda_{max}$ in nm ($\epsilon$ in Lmol$^{-1}$cm$^{-1}$)]: 401 (10150), 505 (273, sh). $\mu_{eff}$(25°C) = 5.5 $\mu_b$. Anal. Calcd for $C_{36}H_{42}N_6O_2P_2F_{12}Mn$: C, 46.21; H, 4.52; N, 8.98; Mn, 5.87. Found: C, 46.42; H, 4.70; N, 8.82; Mn, 5.60.

**[Mn(entnim)(H$^+$)$_2$](PF$_6$)$_2$.** The [Mn(entnim)(H$^+$)$_2$](PF$_6$)$_2$ complex was obtained as an orange microcrystalline solid (67%) after recrystallization. $\Lambda_m = 270\ \Omega^{-1}$ mol$^{-1}$ cm$^2$. UV: 402 (11040), 507 (323, sh). $\mu_{eff}$(25°C) = 5.5 $\mu_b$. Anal. Calcd for $C_{35}H_{40}N_6O_2P_2F_{12}Mn$: C, 45.61; H, 4.38; N, 9.12. Found: C, 45.44; H, 4.56; N, 8.93.

**[Fe(tntnim)(H$^+$)$_2$](PF$_6$)$_2$.** To a mixture of [$Li_2$(tnal)] (500 mg, 0.886 mmol) and [$FeCl_2$(pyridine)$_4$][23] (392 mg, 0.886 mmol) was added ethanol (30 mL). The resultant dark brown suspension was stirred for 10 min. To this suspension was added dropwise over 10 min 1,3-diaminopropane (74.0 $\mu$L, 0.886 mmol) and acetic acid (305 $\mu$L, 5.31 mmol) in ethanol (20 mL). At the end of the addition, all solid material had dissolved. The resultant deep yellow-red solution was stirred for 1 h, and then $NH_4PF_6$ (0.72 g, 4.43 mmol) in ethanol (5 mL) was added. A rusty brown solid was precipitated immediately. The resultant mixture was stirred for 10 min. The solid was then collected, washed

(21) For a recent review of Li coordination chemistry see: Olsher, U.; Izatt, R. M.; Bradshaw, J. S.; Dalley, N. K. *Chem. Rev.* **1991**, *91*, 137−64.

(22) This complex was originally reported by Fraser, C. Ph.D. Thesis, The University of Chicago, 1993, p 255.

(23) Baudisch, O.; Hartung, W. H. *Inorg. Synth.* **1939**, *1*, 184−85.

with ethanol (2 × 5 mL), and dried under high vacuum (0.25 mm) for 3 h. The crude salt was recrystallized from $CH_3CN$−ethanol. Pure $[Fe(tntnim)(H^+)_2](PF_6)_2$ was obtained as maroon needles (492 mg, 59%). $\Lambda_m = 300\ \Omega^{-1}\ mol^{-1}\ cm^2$. UV: 398 (12300), 822 (26). Anal. Calcd for $C_{36}H_{46}N_6O_2P_2F_{12}Fe$: C, 45.96; H, 4.94; N, 8.94. Found: C, 46.20; H, 4.71; N, 8.76.

**$[Fe(entnim)(H^+)_2](PF_6)_2$.** To a mixture of $[Li_2(enal)]$ (1.00 g, 1.82 mmol) and $[FeCl_2(pyridine)_4]$ (0.805 g, 1.82 mmol) was added ethanol (50 mL). The resultant dark brown suspension was stirred for 15 min. To this suspension was added dropwise over 5 min 1,3-diaminopropane (152 $\mu$L, 1.82 mmol) and acetic acid (624 $\mu$L, 10.9 mmol) in ethanol (25 mL). At the end of the addition, all solid material had dissolved. The resultant deep yellow-red solution was stirred for 1 h, and then $NH_4PF_6$ (1.48 g, 9.08 mmol) in ethanol (10 mL) was added, precipitating a rusty brown solid. The resultant mixture was stirred for 10 min, and the solid was collected and washed as above. The crude salt was recrystallized from $CH_3CN$-ethanol. Pure $[Fe(entnim)(H^+)_2](PF_6)_2$ was obtained as a maroon microcrystalline solid (1.28 g, 1.39 mmol, 76%). $\Lambda_m = 270\ \Omega^{-1}\ mol^{-1}\ cm^2$. UV: 398 (10250), 569 (425, sh), 848 (39). Anal. Calcd for $C_{35}H_{44}N_6O_2P_2F_{12}Fe$: C, 45.36; H, 4.80; N, 9.07. Found: C, 45.61; H, 4.60; N, 9.09.

**$[M(diamine)(H^+)_2](PF_6)_2$ Complexes.** Each of the monometallic complexes showed an intense absorption in the electronic spectrum at $\lambda_{max} = 293-307$ nm, $\epsilon = 6.5 \times 10^3\ L\ mol^{-1}\ cm^{-1}$, in $CH_3CN$ solution. The infrared spectrum of the $[Zn(tntnam)(H^+)_2](PF_6)_2$ complex is very similar to that of the $[Zn(tntnim)(H^+)_2](PF_6)_2$ complex. The significant differences in the spectrum of the former include the emergence of a sharp, weak band at 3314 $cm^{-1}$, which is attributed to the N−H stretch of the quaternized amine groups,[24] and the disappearance of the strong band at 1643 $cm^{-1}$, corresponding to the C=N stretch of the imine groups.[24] These differences are assumed to be general for other monometallic imine and amine complexes of similar ligands.

**$[Zn(tntnam)(H^+)_2](PF_6)_2$.** To a stirred solution of $[Zn(tntnim)(H^+)_2](PF_6)_2$ (560 mg, 0.592 mmol) in $CH_3CN$ (5 mL) at 0 °C was added dropwise over 10 min a solution of $NaBH_4$ (22.5 mg, 0.592 mmol) in ethanol (10 mL). The intense yellow color of the imine disappeared rather abruptly near the end of the addition. The resultant very pale yellow solution was warmed to 25 °C over 30 min. Acetic acid (204 $\mu$L, 3.55 mmol) was added to the reaction mixture and a small amount of gas evolution was observed. The solution was heated to 90 °C and the solvents were slowly distilled from the reaction mixture over 1 h until a pale yellow solid precipitated. The suspension was cooled to 25 °C over 20 min. The solid was collected, washed with ethanol (1 × 5 mL), $Et_2O$ (2 × 5 mL), and pentane (2 × 5 mL), and dried under vacuum. The crude salt was recrystallized from methanol on a steam bath. The crystalline complex was collected and washed as above. The $[Zn(tntnam)(H^+)_2](PF_6)_2$ (374 mg, 66%) was obtained as pale yellow needles. $\Lambda_m = 261\ \Omega^{-1}\ mol^{-1}\ cm^2$. $^1H$ NMR (400 MHz, $CD_3CN$): $\delta$ 2.06 (m, 2H); 2.16 (s, 6H); 2.17 (m, 2H); 2.75 (m, 4H); 3.00 (m, 2H); 3.17 (m, 2H); 3.78, 3.28 (syst AB, $J_{AB} = 13.6$ Hz, 4H); 4.13, 3.63 (syst AB, $J_{AB} = 17.7$ Hz, 4H); 4.25, 3.17 (syst AB, $J_{AB} = 11.9$ Hz, 4H); 6.59 (d, $J = 2.0$ Hz, 2H); 6.90 (d, $J = 7.9$ Hz, 2H); 6.92 (d, $J = 2.2$ Hz, 2H); 7.35 (t, $J = 6.2$ Hz, 2H); 7.71 (br s, 4H); 7.71 (td, $J = 7.5$, 1.7 Hz, 2H); 8.92 (d, $J = 4.87$ Hz, 2H). When one drop of $D_2O$ was added to the $^1H$ NMR sample, the broad singlet at $\delta$ 7.71 disappeared. Anal. Calcd for $C_{36}H_{46}N_6O_2P_2F_{12}Zn$: C, 45.50; H, 4.89; N, 8.85; Zn, 6.88. Found: C, 45.28; H, 4.94; N, 8.62; Zn, 6.49.

**$[Co(tntnam)(H^+)_2](PF_6)_2$.** To a stirred solution of $[Co(tntnim)(H^+)_2](PF_6)_2$ (934 mg, 0.994 mmol) in $CH_3CN$ (8 mL) at 0 °C was added dropwise over 20 min a solution of $NaBH_4$ (37.8 mg, 0.994 mmol) in ethanol (15 mL). After approximately half of the borohydride solution had been added, the yellow-orange color of the imine complex changed abruptly to a dark red-orange. At the end of the addition, the resultant red-brown solution was warmed to 25 °C over 30 min, during which time the color changed again to cherry red. The solution was heated to 70 °C over 15 min. Acetic acid (342 $\mu$L, 5.96 mmol) was added to the reaction mixture producing a small amount of gas evolution, and a final color change was observed from red to orange. The reaction mixture was heated to 90 °C and water (3 mL) was added. The solvents were slowly distilled from the solution over 20 min until an orange microcrystalline solid precipitated. The suspension was diluted with a mixture of 50:50 ethanol−water (5 mL) and was cooled to 25 °C over 40 min. The solid was collected, washed with water (3 × 5 mL), ethanol (3 × 5 mL), $Et_2O$ (2 × 5 mL), and pentane (2 × 5 mL), and dried under vacuum. The crude salt (720 mg, 0.763 mmol, 77%) is sufficiently pure for further reactions, but it was recrystallized from methanol prior to characterization. The orange powder was dissolved in a minimum volume of methanol (~50 mL for 0.5 g of crude product) at 50 °C and the solution was filtered. The methanol was slowly distilled from the solution down to approximately half the original volume. Slow cooling to 0 °C resulted in the precipitation of orange needles (403 mg, 0.427 mmol, 43%). $\Lambda_m = 288\ \Omega^{-1}\ mol^{-1}\ cm^2$. UV: 482 (79), 652 (12), 1012 (6). $\mu_{eff}(25°C) = 4.54\ \mu_b$. Anal. Calcd for $C_{36}H_{46}N_6O_2P_2F_{12}Co$: C, 45.81; H, 4.92; N, 8.91. Found: C, 45.72; H, 4.80; N, 8.85.

**$[Mn(tntnam)(H^+)_2](PF_6)_2$.** To a stirred solution of $[Mn(tntnim)(H^+)_2](PF_6)_2$ (0.80 g, 0.85 mmol) in $CH_3CN$ (8 mL) at 0 °C was added dropwise over 15 min a solution of $NaBH_4$ (33 mg, 0.85 mmol) in ethanol (16 mL). After approximately half of the borohydride solution had been added, the intense red color abruptly changed to a very pale yellow. The resultant solution was stirred at 0 °C for 30 min and then warmed to 25 °C over 30 min. Acetic acid (295 $\mu$L, 5.1 mmol) was added to the reaction mixture and gas evolution was observed. The solution was heated to 100 °C and water (5 mL) was added. The solvents were slowly distilled from the reaction mixture over 30 min until a yellow solid precipitated (~5 mL total volume remaining). The suspension was cooled to 25 °C over 30 min. The yellow microcrystalline solid was collected, washed with water (2 × 5 mL) and ethanol (2 × 5 mL), and dried under high vacuum (<0.25 mm) for 2 h. The dry solid was air sensitive and was stored in a glovebox. The crude salt (605 mg, 76%) was recrystallized from acetone−methanol as follows. The yellow solid was dissolved in acetone (~5 mL) at room temperature and the solution was filtered. To the acetone solution was added methanol (30 mL). The resultant mixture was heated to 90 °C and the solvents were slowly distilled from the mixture to induce precipitation. After the solution was reduced to half the original volume, the mixture became cloudy and was allowed to cool to room temperature over 1 h, and then to 0 °C over 1 h. The crystals were collected and washed with cold methanol (~5 mL) and then dried under high vacuum (<0.25 mm). The $[Mn(tntnam)(H^+)_2](PF_6)_2$ (335 mg, 42%) was obtained as pale yellow needles. $\Lambda_m = 271\ \Omega^{-1}\ mol^{-1}\ cm^2$. UV: no d−d bands were observed. Anal. Calcd for $C_{36}H_{46}N_6O_2P_2F_{12}Mn$: C, 46.01; H, 4.94; N, 8.94. Found: C, 46.32; H, 4.75; N, 8.96.

**$[Zn(tnenam)(H^+)_2](PF_6)_2$.** To a stirred solution of $[Zn(tnenim)(H^+)_2](PF_6)_2$ (1.00 g, 1.07 mmol) in $CH_3CN$ (10 mL) at 0 °C was added dropwise over 30 min a solution of $NaBH_4$ (45.0 mg, 1.18 mmol) in ethanol (15 mL). The intense yellow color of the imine disappeared near the end of the addition. Some gas evolution was observed and a pale yellow precipitate was formed during the addition. The resultant mixture was stirred at 0 °C for 1 h and then warmed to 25 °C over 30 min. Acetic acid (406 mL, 7.08 mmol) was added to the reaction mixture and the precipitate dissolved immediately. The resultant pale yellow solution was heated to 90 °C and the solvents were distilled from the reaction mixture over 1 h until a pale yellow solid precipitated. The suspension was cooled to 25 °C over 20 min and was diluted with ethanol (5 mL). The pale yellow solid was collected and washed with ethanol (2 × 5 mL). The crude salt was recrystallized from methanol on a steam bath. The $[Zn(tnenam)(H^+)_2](PF_6)_2$ was obtained as pale yellow needles (0.73 g, 73%). $\Lambda_m = 274\ \Omega^{-1}\ mol^{-1}\ cm^2$. $^1H$ NMR (400 MHz, $CD_3CN$): $\delta$ 2.15 (s, 6H); 2.19 (br s, 2H); 2.23 (m, 2H); 2.88 (m, 4H); 3.17 (m, 4H); 3.87, 3.59 (syst AB, $J_{AB} = 13.7$ Hz, 4H); 4.19, 3.27 (syst AB, $J_{AB} = 12.2$ Hz, 4H); 4.25, 3.74 (syst AB, $J_{AB} = 17.5$ Hz, 4H); 6.62 (d, $J = 1.9$ Hz, 2H); 6.92 (d, $J = 7.9$ Hz, 2H); 6.95 (d, $J = 2.0$ Hz, 2H); 7.32 (t, $J = 6.2$ Hz, 2H); 7.68 (td, $J = 7.7$, 1.7 Hz, 2H); 8.90 (d, $J = 5.3$ Hz, 2H); 8.90 (br s, 2H). When one drop of $D_2O$ was added to the $^1H$ NMR sample, the broad singlets at $\delta$ 8.90 and 2.19 disappeared. Anal. Calcd for $C_{35}H_{44}N_6O_2P_2F_{12}Zn$: C, 44.90; H, 4.75: N, 8.98. Found: C, 45.13; H, 4.68; N, 8.90. Although the

(24) (a) Robinson, J. W., Ed. *Practical Handbook of Spectroscopy*; CRC Press: Boca Raton, FL, 1991; Chapter 5. (b) Silverstein, R. M.; Bassler, G. C. *Spectrometric Identification of Organic Compounds*; John Wiley & Sons: New York, 1963. (c) Gordon, A. J.; Ford, R. A. *The Chemist's Companion*; John Wiley & Sons: New York, 1972.

analytical data and $^1$H NMR spectrum of the $[Zn(tnenam)(H^+)_2](PF_6)_2$ as prepared above indicate that the reduced product is clean, a small amount of contamination (<2%) by partially reduced or unreacted starting material was confirmed by the appearance of the $\pi \rightarrow \pi^*$ transition of the azomethine chromophore of the diimine precursor[8] in the electronic spectrum of the crude product. Complete reduction was effected by resubmitting the crude product for reduction under modified conditions. To a stirred solution of the contaminated product (212.9 mg, 0.228 mmol) in $CH_3CN$ (5 mL) at 0 °C was added dropwise over 10 min a solution of $NaBH_4$ (9.56 mg, 0.251 mmol) in ethanol (2.5 mL). The yellow color pales further and some cloudiness develops at the end of the addition. The mixture was stirred for 1 h at 0 °C and then for 2 h at 25 °C. Acetic acid (86.5 $\mu$L, 1.51 mmol) was added to the reaction mixture, and it was worked up as above. The $[Zn(tnenam)(H^+)_2](PF_6)_2$ (139.5 mg, 65%) was obtained as pale yellow needles after recrystallization. No unreduced components could be detected in the electronic spectrum. A fresh sample of $[Zn(tnenim)(H^+)_2](PF_6)_2$ was reduced under the modified conditions, and the reaction again did not go to completion. Thus, in order to effect the complete reduction of the imine complex, two treatments with borohydride are necessary.

**$[Co(tnenam)(H^+)_2](PF_6)_2$.** The $[Co(tnenim)(H^+)_2](PF_6)_2$ was reduced by the method used for the preparation of $[Zn(tnenam)(H^+)_2](PF_6)_2$. The color changes were similar to those observed in the preparation of $[Co(tntnam)(H^+)_2](PF_6)_2$. The $[Co(tnenam)(H^+)_2](PF_6)_2$ was obtained as orange needles after the recrystallization from methanol. Yield: 38%. $\Lambda_m = 280\ \Omega^{-1}\ mol^{-1}\ cm^2$. UV: 444 (63), 485 (49), 534 (23), 647 (6), 1001 (4). $\mu_{eff}(25°C) = 4.6\ \mu_b$. Anal. Calcd for $C_{35}H_{44}N_6O_2P_2F_{12}Co$: C, 45.21; H, 4.78; N, 9.04. Found: C, 45.54; H, 4.82; N, 9.13.

**$[Zn(entnam)(H^+)_2](PF_6)_2$.** To a stirred solution of $[Zn(entnim)(H^+)_2](PF_6)_2$ (0.55 g, 0.59 mmol) in $CH_3CN$ (4 mL) at 0 °C was added dropwise over 10 min a solution of $NaBH_4$ (24.7 mg, 0.649 mmol) in ethanol (8 mL). After approximately half of the borohydride solution had been added, a fluffy white precipitate formed. The resultant pale yellow suspension was stirred for 1 h at 0 °C, and the color faded. The nearly colorless suspension was warmed to 25 °C and stirred for 2 h. Acetic acid (230 $\mu$L, 3.89 mmol) was added to the reaction mixture, and some gas evolution was observed. The suspension was heated to 100 °C and water (3 mL) was added. The white solid dissolved momentarily, and a microcrystalline solid precipitated almost immediately. Water (2 mL) was added and the solvents were distilled from the reaction mixture over 1 h until the total volume was <5 mL. The suspension was cooled to 25 °C over 30 min and the pale yellow solid was collected, washed with water (2 × 5 mL), ethanol (3 × 5 mL), $Et_2O$ (2 × 5 mL), and pentane (2 × 5 mL), and dried under vacuum. The pale yellow product was recrystallized from $CH_3CN$−ethanol as follows. The crude salt was dissolved in a minimum amount of $CH_3CN$ (~10 mL for 0.5 g of crude product) on the steam bath. To the $CH_3CN$ solution was added several aliquots of ethanol (~4 × 10 mL) over several hours. The crystalline complex was collected and washed as above. The $[Zn(entnam)(H^+)_2](PF_6)_2$ (0.47 g, 85%) was obtained as pale yellow plates. $\Lambda_m = 269\ \Omega^{-1}\ mol^{-1}\ cm^2$. $^1$H NMR (400 MHz, $CD_3CN$): $\delta$ 2.14 (br m, 4H); 2.14 (s, 6H); 2.84 (m, 4H); 3.06 (m, 4H); 3.80, 3.36 (syst AB, $J_{AB}$ = 13.4 Hz, 4H); 3.98, 3.82 (syst AB, $J_{AB}$ = 18.1 Hz, 4H); 4.03, 3.49 (syst AB, $J_{AB}$ = 11.9 Hz, 4H); 6.64 (d, 2.0 Hz, 2H); 6.86 (d, 2.2 Hz, 2H); 6.96 (d, 7.5 Hz, 2H); 7.33 (t, $J$ = 6.6 Hz, 2H); 7.74 (td, $J$ = 7.7 Hz, 1.9 Hz, 2H); 8.85 (d, $J$ = 5.3 Hz, 2H); 11.2 (br s, 2H). When one drop of $D_2O$ was added to the $^1$H NMR sample, the broad singlet at $\delta$ 11.2 disappeared and the broad multiplet at $\delta$ 2.14 sharpened into a quintet at $\delta$ 2.17 ($J$ = 6.6 Hz, 2H). Anal. Calcd for $C_{35}H_{44}N_6O_2P_2F_{12}Zn$: C, 44.90; H, 4.75; N, 8.98. Found: C, 45.04; H, 4.65; N, 8.61.

**$[Co(entnam)(H^+)_2](PF_6)_2$.** The $[Co(entnim)(H^+)_2](PF_6)_2$ was reduced by the method described for the preparation of $[Zn(entnam)(H^+)_2](PF_6)_2$. The color changes were similar to those observed in the preparation of $[Co(tntnam)(H^+)_2](PF_6)_2$. The $[Co(entnam)(H^+)_2](PF_6)_2$ was obtained as pink plates after recrystallization from $CH_3CN$−ethanol. Yield: 61%. $\Lambda_m = 275\ \Omega^{-1}\ mol^{-1}\ cm^2$. UV: 477 (65), 994 (12). $\mu_{eff}(25°C) = 4.5\ \mu_b$. Anal. Calcd for $C_{35}H_{44}N_6O_2P_2F_{12}Co$: C, 45.21; H, 4.78; N, 9.04. Found: C, 45.34; H, 4.82; N, 8.92.

**$[Mn(entnam)(H^+)_2](PF_6)_2$.** The $[Mn(entnam)(H^+)_2](PF_6)_2$ complex was reduced by the method described for the preparation of $[Zn(entnam)(H^+)_2](PF_6)_2$. The color changes were similar to those observed in the preparation of $[Mn(tntnam)(H^+)_2](PF_6)_2$. The $[Mn(entnam)(H^+)_2](PF_6)_2$ was obtained as a yellow microcrystalline solid after recrystallization from acetone-ethanol (22%). $\Lambda_m = 256\ \Omega^{-1}\ mol^{-1}\ cm^2$. UV: 498 (10). Anal. Calcd for $C_{35}H_{44}N_6O_2P_2F_{12}Mn$: C, 45.41; H, 4.80; N, 9.08. Found: C, 45.52; H, 4.81; N, 8.90.

**$[Zn(enenam)(H^+)_2](PF_6)_2$.** The $[Zn(enenim)(H^+)_2](PF_6)_2$ was reduced by the method described for the preparation of $[Zn(tntnam)(H^+)_2](PF_6)_2$. The $[Zn(enenam)(H^+)_2](PF_6)_2$ was obtained as yellow plates after recrystallization from $CH_3CN$−ethanol. Yield: 81%. $\Lambda_m = 268\ \Omega^{-1}\ mol^{-1}\ cm^2$. $^1$H NMR (400 MHz, $CD_3CN$): $\delta$ 2.14 (br s, 4H); 2.14 (s, 6H); 2.92 (m, 4H); 3.33 (s, 4H); 3.61 (d, $J$ = 12.1 Hz, 2H); 3.85 (d, $J$ = 14.1 Hz, 2H); 3.98 (m, 4H); 4.16 (m, 4H); 6.67 (d, $J$ = 1.5 Hz, 2H); 6.90 (d, $J$ = 2.0 Hz, 2H); 7.03 (d, $J$ = 7.87 Hz, 2H); 7.33 (t, $J$ = 6.6 Hz, 2H); 7.73 (td, $J$ = 7.7, 1.7 Hz, 2H); 8.84 (d, $J$ = 4.5 Hz, 2H). When a drop of $D_2O$ was added to the $^1$H NMR sample the broad singlet at $\delta$ 2.14 disappeared. Anal. Calcd for $C_{34}H_{42}N_6O_2P_2F_{12}Zn$: C, 44.28; H, 4.60; N, 9.12. Found: C, 44.90; H, 4.66; N, 9.16.

**$[Co(enenam)(H^+)_2](PF_6)_2$.** The $[Co(enenim)(H^+)_2](PF_6)_2$ was reduced by the method described for the preparation of $[Co(tntnam)(H^+)_2](PF_6)_2$. The $[Co(enenam)(H^+)_2](PF_6)_2$ was obtained as salmon-colored plates after recrystallization from $CH_3CN$−ethanol. Yield: 65%. $\Lambda_m = 280\ \Omega^{-1}\ mol^{-1}\ cm^2$. UV: 472 (53), 981 (7). $\mu_{eff}(25°C) = 4.4\ \mu_b$. Anal. Calcd for $C_{34}H_{42}N_6O_2P_2F_{12}Co$: C, 44.59; H, 4.63; N, 9.18. Found: C, 44.90; H, 4.77; N, 9.31.

**$[Co(diamine)(H^+)_2](PF_6)_3$ Complexes.** All of the $[Co(diamine)(H^+)_2](PF_6)_3$ complexes were prepared by the oxidation of the corresponding $[Co(diamine)(H^+)_2](PF_6)_2$ complexes with $[Cp_2Fe]PF_6$. The general method is described for the preparation of $[Co(tntnam)(H^+)_2](PF_6)_3$. The Co(III) derivatives of the entnam and enenam ligands were also prepared by the $NaBH_4$ reduction of the corresponding monometallic Co(III) imine complexes. All complexes showed an intense absorption in the electronic spectrum at $\lambda_{max}$ = 415−440 nm ($\epsilon$ = 1400−4000 L $mol^{-1}\ cm^{-1}$) in $CH_3CN$ solution which is assigned to the Co(III)−phenolate charge transfer transition.[8,25]

**$[Co(tntnam)(H^+)_2](PF_6)_3$.** To a stirred solution of the $[Co(tntnam)(H^+)_2](PF_6)_2$ (360.5 mg, 0.382 mmol) in $CH_3CN$ (4 mL) was added $[Cp_2Fe]PF_6$ (139.1 mg, 0.420 mmol) in $CH_3CN$ (6 mL). The resultant green-black solution was stirred approximately 10 min, and then was opened to the air and concentrated to dryness. The residue was triturated with $Et_2O$ (3 × 5 mL) in order to remove $Cp_2Fe$. The residue was collected, washed with ethanol (1 × 5 mL), $Et_2O$ (3 × 5 mL), and pentane (3 × 5 mL), and dried under vacuum. The black solid was recrystallized from $CH_3CN$−ethanol−$Et_2O$ as follows. The crude salt was dissolved in $CH_3CN$ (~1 mL), and aliquots of equal volumes of ethanol and $Et_2O$ (~5 × 5 mL of each) were added over several days. The $[Co(tntnam)(H^+)_2](PF_6)_3$ (0.32 g, 77%) was obtained as black needles. $\Lambda_m = 361\ \Omega^{-1}\ mol^{-1}\ cm^2$. UV: 438 (3930), 565 (1750), 628 (1550). $^1$H NMR (400 MHz, $CD_3CN$): $\delta$ 2.11 (s, 6H); 2.23 (m, 2H); 2.45 (m, 2H); 2.66 (m, 4H); 3.19 (m, 6H); 3.43 (m, 2H); 3.66 (m, 2H); 4.08 (d, $J$ = 13.0 Hz, 2H); 4.62, 3.87 (syst AB, $J_{AB}$ = 19.0 Hz, 4H); 6.76 (d, $J$ = 2.0 Hz, 2H); 6.98 (d, $J$ = 2.0 Hz, 2H); 7.10 (br s, 2H); 7.15 (d, $J$ = 7.9 Hz, 2H); 7.34 (br s, 2H); 7.59 (t, $J$ = 6.3 Hz, 2H); 7.92 (td, $J$ = 7.7 , 1.4 Hz, 2H); 8.96 (d, $J$ = 5.5 Hz, 2H). When one drop of $D_2O$ was added to the $^1$H NMR sample the broad singlets at $\delta$ 7.34 and 7.10 disappeared. Anal. Calcd for $C_{36}H_{46}N_6O_2P_3F_{18}Co$: C, 39.71; H, 4.27; N, 7.72. Found: C, 39.50; H, 4.11; N, 7.35.

**$[Co(tnenam)(H^+)_2](PF_6)_3 \cdot CH_3CN$.** The complex was obtained as black needles. Yield: 76%. Crystals suitable for X-ray structure determination were obtained by crystallizing the $[Co(tnenam)(H^+)_2](PF_6)_3$ complex by vapor diffusion of $Et_2O$ into an $CH_3CN$ solution of the complex. These crystals retained one molecule of $CH_3CN$ as a solvent of crystallization. $\Lambda_m = 359\ \Omega^{-1}\ mol^{-1}\ cm^2$. UV: 432 (3780), 606 (1270). $^1$H NMR (300 MHz, $CD_3CN$): $\delta$ 2.12 (s, 6H); 2.44 (m, 2H); 2.66 (t, $J$ = 6.5 Hz, 4H); 3.28 (m, 4H); 3.59 (m, 4H); 3.95 (m, 6H); 4.61 (d, $J$ = 18.9 Hz, 2H); 6.75 (s, 2H); 6.99 (s, 2H); 7.20 (d, $J$ = 7.8 Hz, 2H); 7.58 (t, $J$ = 6.5 Hz, 2H); 7.76 (br s, 2H); 7.93 (td, $J$ = 7.7, 1.0 Hz, 2H); 8.43 (br s, 2H); 8.82 (d, $J$ = 5.7 Hz, 2H). When a

(25) (a) Garbett, K.; Gillard, R. D. *J. Chem. Soc. A* **1968**, 979−87. (b) Yamamoto, Y.; Kudo, H.; Toyota, E. *Bull. Chem. Soc. Jpn.* **1983**, *56*, 1051−56.

drop of $D_2O$ was added to the $^1H$ NMR sample the broad singlets at $\delta$ 8.43 and 7.76 disappeared. Anal. Calcd for $C_{35}H_{44}N_6O_2P_3F_{18}Co{\cdot}CH_3CN$: C, 39.83; H, 4.25; N, 8.78. Found: C, 39.61; H, 4.00; N, 8.65.

**[Co(entnam)($H^+$)$_2$]($PF_6$)$_3$. Method 1:** The complex was prepared by the method described for the preparation of [Co(tntnam)($H^+$)$_2$]($PF_6$)$_3$. The [Co(entnam)($H^+$)$_2$]($PF_6$)$_3$ (53%) was obtained as dark maroon blocks. **Method 2:** To a stirred solution of [Co(entnim)($H^+$)$_2$]($PF_6$)$_3$ (200 mg, 0.187 mmol) in $CH_3CN$ (2 mL) at 0 °C was added dropwise a solution of $NaBH_4$ (7.81 mg, 0.205 mmol) in ethanol (4 mL). The yellow-maroon color of the imine complex disappeared at the end of the addition. The resultant dark maroon solution was stirred for 30 min at 0 °C, and then was warmed to 25 °C over 15 min. Acetic acid (70.7 $\mu$L, 1.23 mmol) was added to the reaction mixture and a small amount of gas evolution was observed. The solution was heated to 100 °C and water (5 mL) was added. The solvents were slowly distilled from the reaction mixture over 30 min until a dark solid precipitated. The suspension was cooled to 25 °C over 20 min. The solid was collected, washed with warm water (2 × 5 mL), $Et_2O$ (4 × 5 mL), and pentane (3 × 5 mL), and dried under vacuum. The crude product (163.5 mg, 81%) was recrystallized from $CH_3CN$−ethanol−$Et_2O$. The [Co(entnam)($H^+$)$_2$]($PF_6$)$_3$ (143 mg, 71%) was obtained as maroon blocks. $\Lambda_m$ = 373 $\Omega^{-1}$ mol$^{-1}$ cm$^2$. UV: 419 (2120), 544 (980). $^1H$ NMR (500 MHz, $CD_3CN$): $\delta$ 2.16 (s, 6H); 2.23 (br m, 6H); 3.20 (m, 6H); 3.50 (m, 2H); 3.61, 3.45 (syst AB, $J_{AB}$ = 14.5 Hz, 4H); 3.90, 3.53 (syst AB, $J_{AB}$ = 12.7 Hz, 4H); 4.52, 4.37 (syst AB, $J_{AB}$ = 19.0 Hz, 4H); 6.83 (s, 2H); 6.85 (s, 2H); 7.31 (d, $J$ = 7.8 Hz, 2H); 7.52 (t, $J$ = 6.6 Hz, 2H); 7.96 (t, $J$ = 7.4 Hz, 2H); 8.45 (d, $J$ = 5.8 Hz, 2H). When a drop of $D_2O$ was added to the $^1H$ NMR sample, the broad multiplet at $\delta$ 2.23 was resolved into a new multiplet of lower intensity (2H). Anal. Calcd for $C_{35}H_{44}N_6O_2P_3F_{18}Co$: C, 39.11; H, 4.14; N, 7.82. Found: C, 39.04; H, 3.85; N, 7.88.

**[Co(enenam)($H^+$)$_2$]($PF_6$)$_3$. Method 1:** The crude product had the same UV and $^1H$ NMR spectra as the product obtained by Method 2 (see below). Pure product was not isolated. **Method 2:** The complex was obtained as maroon blocks. Yield: 52%. $\Lambda_m$ = 375 $\Omega^{-1}$ mol$^{-1}$ cm$^2$. UV: 415 (1420), 513 (550), 577 (410). $^1H$ NMR (500 MHz, $CD_3CN$): $\delta$ 2.17(br m, 4H); 2.17(s, 6H); 3.39 (m, 12H); 4.15, 3.91 (syst AB, $J_{AB}$ = 13.0 Hz, 4H); 4.68, 4.45 (syst AB, $J_{AB}$ = 18.8 Hz, 4H); 6.86 (s, 2H); 6.88 (s, 2H); 7.36 (d, $J$ = 7.8 Hz, 2H); 7.47 (t, $J$ = 6.5 Hz, 2H); 7.97 (t, $J$ = 7.7 Hz, 2H); 8.17 (d, $J$ = 3.2 Hz, 2H). Anal. Calcd for $C_{34}H_{42}N_6O_2P_3F_{18}Co$: C, 38.50; H, 4.00; N, 7.93. Found: C, 38.58; H, 4.18; N, 7.81.

**Bimetallic Complexes. [Zn(diamine)ZnCl]$PF_6$ Complexes.** All of the [Zn(diamine)ZnCl]$PF_6$ complexes were prepared by the general method described for [Zn(tntnam)ZnCl]$PF_6$. All dechlorinated complexes were prepared by the general method described for [Zn(tntnam)Zn]($PF_6$)$_2$. All of the chloro complexes showed an intense absorption in the electronic spectrum at $\lambda_{max}$ = 300 nm ($\epsilon$ = 5500−6500 L mol$^{-1}$ cm$^{-1}$) in $CH_3CN$ solutions. All reported $^1H$ NMR spectra were obtained 24 h after sample preparation. Isomer ratios are based on the 5-pyridyl proton resonances unless denoted otherwise. The secondary amine protons were not located in the $^1H$ NMR spectra for any of these complexes. The infrared spectrum of the [Zn(tntnam)ZnCl]$PF_6$ complex is very similar to that of the [Zn(tntnim)ZnCl]$PF_6$ complex. The significant differences in the spectrum of the former complex include the emergence of a sharp, weak band at 3290 cm$^{-1}$, which is attributed to the N−H stretch of the secondary amine groups,[24] and the disappearance of the strong band at 1627 cm$^{-1}$, corresponding to the C=N stretch of the imine groups.[24] These differences are assumed to be general for other bimetallic imine and amine complexes of similar ligands.

**[Zn(tntnam)ZnCl]$PF_6$.** To a stirred solution of [Zn(tntnam)($H^+$)$_2$]($PF_6$)$_2$ (150 mg, 0.158 mmol) in $CH_3CN$ (1 mL) was added $ZnCl_2$ (22.0 mg, 0.158 mmol) in methanol (2.5 mL). To the resultant pale yellow mixture was added dropwise over 5 min lithium hydroxide monohydrate (13.5 mg, 0.316 mmol) in methanol (2.5 mL). The resultant colorless solution was stirred for 5 min, and $NH_4PF_6$ (130 mg, 0.79 mmol) in methanol (5 mL) was added to it. The reaction mixture was concentrated to dryness under reduced pressure. The residue was dissolved in ethanol (3 mL) on the steam bath. The resultant solution was cooled to 0 °C over 2 h, and white crystals precipitated. The crystalline [Zn(tntnam)ZnCl]$PF_6$ (116 mg, 81%) was washed with cold ethanol (2 × 3 mL, 0 °C), $Et_2O$ (2 × 3 mL), and pentane (2 × 3 mL) and dried under vacuum. $\Lambda_m$ = 117 $\Omega^{-1}$ mol$^{-1}$ cm$^2$. $^1H$ NMR (400 MHz, acetone-$d_6$): major isomer, $\delta$ 1.93 (m, 1H); 2.08 (s, 3H); 2.10 (s, 3H); 2.20 (m, 1H); 2.35 (m, 1H); 2.94 (m, 11H); 3.41 (d, $J$ = 12.3 Hz, 1H); 3.60 (m, 1H); 3.91 (d, $J$ = 17.1 Hz, 1H); 4.18 (m, 2H); 4.45 (m, 4H); 4.75 (m, 1H); 6.52 (d, $J$ = 2.2 Hz, 1H); 6.65 (d, $J$ = 2.0 Hz, 1H); 6.83 (d, $J$ = 2.2 Hz, 1H); 6.86 (d, $J$ = 2.4 Hz, 1H); 6.96 (d, $J$ = 7.9 Hz, 1H); 7.24 (d, $J$ = 7.9 Hz, 1H); 7.31 (t, $J$ = 6.2 Hz, 1H); 7.38 (t, $J$ = 6.6 Hz, 1H); 7.67 (td, $J$ = 7.7, 1.7 Hz, 1H); 7.84 (td, $J$ = 7.7, 1.7 Hz, 1H); 8.92 (d, $J$ = 4.9 Hz, 1H); 9.26 (d, $J$ = 4.9 Hz, 1H). There is evidence of two other isomers at the following positions: second isomer, $\delta$ 2.08 (s, 3H); 2.12 (s, 3H); 6.46 (d, $J$ = 2.2 Hz, 1H); 6.74 (s, 1H); 6.76 (s, 1H); 6.89 (m, 2H); 7.18 (m, 1H); 7.47 (m, 2H); 7.59 (td, $J$ = 7.7, 1.7 Hz, 1H); 8.00 (td, $J$ = 7.7, 1.7 Hz, 1H); 8.78 (d, $J$ = 5.0 Hz, 1H); 9.24 (d, $J$ = 5.1 Hz, 1H); third isomer, $\delta$ 9.31 (d, $J$ = 5.2 Hz). The ratio of isomers is 90:8:2 after 24 h. The first and second isomers each show two singlets (first isomer, 2.10 and 2.08 ppm; second isomer, 2.12 and 2.08 ppm) corresponding to the *p*-tolyl methyl groups and two doublets (first isomer, 9.26 and 8.92 ppm; second isomer, 9.24 and 8.78 ppm) corresponding to the 5-pyridyl protons, confirming the magnetic inequivalence of similar protons in these isomers. This result is consistent with $C_1$ symmetry for each isomer. The third isomer is only identified by one doublet (9.31 ppm), and therefore its symmetry cannot be determined from the $^1H$ NMR spectrum. Anal. Calcd for $C_{36}H_{44}N_6O_2PF_6ClZn_2$: C, 47.83; H, 4.92; N, 9.30; Cl, 3.92. Found: C, 47.47; H, 4.91; N, 9.01; Cl, 3.71.

**[Zn(tntnam)Zn]($PF_6$)$_2$.** An excess of $AgPF_6$ was added to the [Zn(tntnam)ZnCl]$PF_6$ in acetone-$d_6$ (700 $\mu$L) in an NMR tube, and the resultant mixture was shaken to precipitate AgCl. $^1H$ NMR (400 MHz, acetone-$d_6$): major isomer, $\delta$ 1.95 (m, 2H); 2.10 (s, 3H); 2.13 (s, 3H); 2.36 (m, 2H); 2.65 (m, 1H); 2.97 (m, 5H); 3.35 (m, 5H); 4.24 (m, 9H); 6.58 (d, $J$ = 2.2 Hz, 1H); 6.73 (d, $J$ = 2.0 Hz, 1H); 6.92 (d, $J$ = 2.2 Hz, 1H); 6.97 (d, $J$ = 2.4 Hz, 1H); 7.01 (d, $J$ = 7.8 Hz, 1H); 7.32 (m, 2H); 7.46 (t, $J$ = 6.1 Hz, 1H); 7.71 (td, $J$ = 7.7, 1.7 Hz, 1H); 7.92 (td, $J$ = 7.7, 1.7 Hz, 1H); 8.89 (d, $J$ = 4.1 Hz, 1H); 9.13 (d, $J$ = 4.6 Hz, 1H). There is evidence of two other isomers at the following positions: second isomer, $\delta$ 2.11 (s, 6H); 6.66 (d, $J$ = 1.8 Hz, 2H); 6.88 (d, $J$ = 2.2 Hz, 2H); 7.22 (d, $J$ = 8.0 Hz, 2H); 7.38 (m, 2H); 7.85 (m, 2H); 8.88 (m, 2H); third isomer, $\delta$ 2.12 (s, 6H); 6.66 (m, 2H); 6.96 (m, 2H); 7.22 (m, 2H); 7.46 (m, 2H); 7.89 (m, 2H); 8.93 (d, $J$ = 5.5 Hz, 2H). The ratio of isomers is 81:7:12 after 24 h. In the spectrum of the first isomer, the appearance of two singlets at 2.13 and 2.10 ppm, corresponding to the protons on the *p*-tolyl methyl groups, and two doublets at 9.13 and 8.89 ppm, corresponding to the 5-pyridyl protons, confirms the magnetic inequivalence of similar protons in this isomer, and is consistent with $C_1$ symmetry. The second and third isomers each show one singlet corresponding to the *p*-tolyl methyl protons (2.11 and 2.12 ppm, respectively) and one doublet corresponding to the 5-pyridyl protons (8.88 and 8.93 ppm, respectively), confirming the magnetic equivalence of similar protons in these isomers. These results are consistent with $C_2$ symmetry, which is achieved when the chloride is removed.

**[Zn(tnenam)ZnCl]$PF_6$.** The white powder obtained by recrystallization of the crude product from 95% ethanol was recrystallized from acetone−ethanol. The [Zn(tnenam)ZnCl]$PF_6$ was obtained as fine white plates (79%). $\Lambda_m$ = 102 $\Omega^{-1}$ mol$^{-1}$ cm$^2$. $^1H$ NMR (400 MHz, acetone-$d_6$): major isomer, $\delta$ 1.87 (m, 2H); 2.08 (s, 3H); 2.13 (s, 3H); 2.42 (m, 1H); 2.54 (m, 1H); 2.85 (m, 3H); 3.45 (m, 9H); 4.27 (m, 4H); 4.58 (m, 2H); 6.48 (d, $J$ = 2.2 Hz, 1H); 6.76 (s, 1H); 6.79 (s, 1H); 6.87 (m, 2H); 7.23 (m, 1H); 7.47 (m, 2H); 7.62 (td, $J$ = 7.7, 1.7 Hz, 1H); 8.80 (td, $J$ = 7.7, 1.7 Hz, 1H); 8.80 (m, 1H); 9.20 (d, $J$ = 4.6 Hz, 1H). There is evidence of at least two other isomers at the following positions: second isomer, $\delta$ 2.08 (s, 3H); 2.16 (2, 3H); 6.95 (d, $J$ = 8.0 Hz, 1H); 7.30 (m, 1H); 7.46 (m, 1H); 7.54 (d, $J$ = 7.6 Hz, 1H); 7.67 (td, $J$ = 7.7, 1.7 Hz, 1H); 8.01 (td, $J$ = 7.7, 1.7 Hz, 1H); 8.80 (m, 1H); 9.43 (d, $J$ = 4.1 Hz, 1H); third isomer, $\delta$ 2.07 (s, 3H); 2.13 (s, 3H); 8.44 (m, 1H); 9.26 (m, 1H). The ratio of isomers is 67:22:11 after 24 h. The peaks at 9.26 and 8.44 ppm, corresponding to the two 5-pyridyl protons of the third isomer, are very broad at 20 °C. As the temperature is lowered to −60 °C, these peaks are resolved into doublets ($J$ = 6.0 and 5.7 Hz, respectively). For each isomer, two singlets are

observed, corresponding to the *p*-tolyl methyl protons (first isomer, 2.13 and 2.08 ppm; second isomer, 2.16 and 2.08 ppm; third isomer, 2.13 and 2.07 ppm), and two doublets are observed, corresponding to the 5-pyridyl protons (first isomer, 9.20 and 8.80 ppm; second isomer, 9.43 and 8.80 ppm; third isomer, 9.26 and 8.44 ppm), confirming the magnetic inequivalence of similar protons in each isomer. The result is consistent with $C_1$ symmetry for each isomer. Anal. Calcd for $C_{35}H_{42}N_6O_2PF_6ClZn_2$: C, 47.23; H, 4.77; N, 9.45; Cl, 3.98. Found: C, 47.02; H, 4.90; N, 9.28; Cl, 3.77.

**[Zn(tnenam)Zn](PF$_6$)$_2$.** $^1$H NMR (400 MHz, acetone-$d_6$): major isomer, $\delta$ 2.08 (s, 3H); 2.18 (s, 3H); 3.10 (m, 22H); 6.52 (d, $J$ = 2.1 Hz, 1H); 6.96 (m, 4H); 7.33 (m, 1H); 7.57 (m, 1H); 7.70 (m, 2H); 8.12 (td, $J$ = 7.7, 1.7 Hz, 1H); 8.89 (d, $J$ = 4.6 Hz, 1H); 9.16 (d, $J$ = 4.9 Hz, 1H). There is evidence of at least two other isomers at the following positions: second isomer, $\delta$ 2.13 (s, 6H); 3.10 (m, 22H); 6.70 (d, $J$ = 1.7 Hz, 2H); 6.92 (d, $J$ = 2.0 Hz, 2H); 7.28 (d, $J$ = 8.0 Hz, 2H); 7.43 (m, 2H); 7.88 (td, $J$ = 7.7, 1.7 Hz, 2H); 8.86 (d, $J$ = 5.1 Hz, 2H); third isomer, $\delta$ 2.12 (s, 6H); 3.10 (m, 22H); 6.75 (s, 2H); 6.96 (m, 2H); 7.38 (d, $J$ = 7.8 Hz, 2H); 7.47 (t, $J$ = 6.3 Hz, 2H); 7.94 (td, $J$ = 7.7, 1.7 Hz, 2H); 8.84 (m, 2H). The ratio of isomers is 25:51:24 after 24 h. In the spectrum of the first isomer, the appearance of two singlets at 2.18 and 2.08 ppm corresponding to the *p*-tolyl methyl protons and two doublets at 9.16 and 8.89 ppm corresponding to the 5-pyridyl protons confirms the magnetic inequivalence of similar protons in this isomer, and is consistent with $C_1$ symmetry. The second and third isomers each show one singlet, corresponding to the *p*-tolyl methyl protons (2.13 and 2.12 ppm respectively), and one doublet, corresponding to the 5-pyridyl protons (8.86 and 8.84 ppm, respectively), confirming the magnetic equivalence of similar protons in these isomers. This result is consistent with $C_2$ symmetry, which is achieved when the chloride is removed. A fourth species is observed at the following positions: $\delta$ 8.6 (m), 7.8 (m), 7.65 (m), 7.2 (m), 7.05 (m), 6.8 (s), 2.11 (s), 2.09 (s). This species consistently integrates as approximately 5% of the total spectrum over 24 h.

**[Zn(entnam)ZnCl]PF$_6$.** The crude product was insoluble in ethanol and was therefore recrystallized from acetone−ethanol. The [Zn(entnam)ZnCl]PF$_6$ was obtained as white plates (59%). $\Lambda_m$ = 116 $\Omega^{-1}$ mol$^{-1}$ cm$^2$. $^1$H NMR (400 MHz, acetone-$d_6$): $\delta$ 2.09 (s, 3H); 2.12 (s, 3H); 2.64 (m, 2H); 3.04 (m, 6H); 3.33 (m, 3H); 3.62 (m, 1H); 3.63 (d, $J$ = 11.8 Hz, 1H); 3.94 (d, $J$ = 13.2 Hz, 1H); 4.03 (d, $J$ = 12.0 Hz, 1H); 4.21 (m, 3H); 4.40 (m, 2H); 4.53 (d, $J$ = 17.6 Hz, 1H); 4.70 (t, $J$ = 12.5 Hz, 1H); 6.59 (d, $J$ = 2.2 Hz, 1H); 6.78 (d, $J$ = 2.4 Hz, 1H); 6.87 (d, $J$ = 2.2 Hz, 1H); 6.98 (d, $J$ = 7.9 Hz, 1H); 7.28 (t, $J$ = 6.0 Hz, 1H); 7.43 (m, 2H); 7.66 (td, $J$ = 7.7, 1.7 Hz, 1H); 7.94 (td, $J$ = 7.7, 1.6 Hz, 1H); 8.69 (d, $J$ = 4.7 Hz, 1H); 9.05 (d, $J$ = 5.1 Hz, 1H). Only one isomer was observed. The appearance of two singlets at 2.12 and 2.09 ppm, corresponding to the *p*-tolyl methyl protons, and two doublets at 9.05 and 8.69 ppm, corresponding to the 5-pyridyl protons, confirms the magnetic inequivalence of similar protons in this complex and is consistent with $C_1$ symmetry. Anal. Calcd for $C_{35}H_{42}N_6O_2PF_6ClZn_2$: C, 47.23; H, 4.77; N, 9.45; Cl, 3.98. Found: C, 47.47; H, 4.89; N, 9.33; Cl, 3.77.

**[Zn(entnam)Zn](PF$_6$)$_2$.** $^1$H NMR (400 MHz, acetone-$d_6$): major isomer, $\delta$ 2.11 (s, 3H); 2.14 (s, 3H); 2.66 (m, 1H); 3.35 (m, 11H); 3.74 (d, $J$ = 12.2 Hz, 1H); 4.03 (d, $J$ = 13.4 Hz, 1H); 4.22 (m, 6H); 4.41 (d, $J$ = 13.2 Hz, 1H); 4.56 (d, $J$ = 17.8 Hz, 1H); 6.66 (d, $J$ = 2.2 Hz, 1H); 6.87 (d, $J$ = 2.0 Hz, 2H); 6.97 (d, $J$ = 2.2 Hz, 1H); 7.04 (d, $J$ = 8.0 Hz, 1H); 7.27 (t, $J$ = 6.3 Hz, 1H); 7.52 (m, 2H); 7.69 (td, $J$ = 7.7, 1.7 Hz, 1H); 8.03 (td, $J$ = 7.7, 1.6 Hz, 1H); 8.61 (d, $J$ = 5.2 Hz, 1H); 9.00 (d, $J$ = 5.1 Hz, 1H). There is evidence of at least one other isomer at the following positions: $\delta$ 2.13 (s, 6H); 6.55 (d, $J$ = 0.67 Hz, 2H); 6.87 (m, 2H); 7.04 (m, 2H); 7.30 (m, 2H); 7.64 (td, $J$ = 7.7, 1.7 Hz, 2H); 8.99 (d, $J$ = 0.54 Hz, 2H). The ratio of isomers is 90:10 after 24 h. In the spectrum of the major isomer, the appearance of two singlets at 2.14 and 2.11 ppm, corresponding to the *p*-tolyl methyl protons, and two doublets at 9.00 and 8.61 ppm, corresponding to the 5-pyridyl protons, confirms the magnetic inequivalence of similar protons in this isomer, and is consistent with $C_1$ symmetry. The minor isomer shows one singlet at 2.13 ppm corresponding to the *p*-tolyl methyl protons, and one doublet at 8.99 ppm corresponding to the 5-pyridyl protons, confirming the magnetic equivalence of similar protons in this isomer. This result is consistent with $C_2$ symmetry.

**[Zn(enenam)ZnCl]PF$_6$.** The crude product was insoluble in ethanol, and was therefore recrystallized from acetone−ethanol. The [Zn(enenam)ZnCl]PF$_6$ was obtained as white plates (80%). Crystals suitable for X-ray structure determination were obtained by crystallizing the [Zn(enenam)ZnCl]PF$_6$ complex by vapor diffusion of ethanol into a $CH_3CN$ solution of the complex. $\Lambda_m$ = 122 $\Omega^{-1}$ mol$^{-1}$ cm$^2$. $^1$H NMR (400 MHz, acetone-$d_6$): major isomer, $\delta$ 2.04 (s, 6H); 3.10 (m, 4H); 3.36 (m, 2H); 3.51 (m, 6H); 3.95 (m, 2H); 4.24 (m, 4H); 4.69 (d, $J$ = 11.8 Hz, 2H); 6.52 (s, 2H); 6.77 (s, 2H); 7.12 (d, $J$ = 7.9 Hz, 2H); 7.25 (t, $J$ = 6.1 Hz, 2H); 7.65 (td, $J$ = 7.7, 1.7 Hz, 2H); 8.64 (br s, 2H). There is evidence of at least one other isomer at the following positions: minor isomer, $\delta$ 1.95 (s, 3H); 2.11 (s, 3H); 6.41 (s, 1H); 6.67 (s, 1H); 6.70 (s, 1H); 6.89 (s, 1H); 7.12 (m, 1H); 7.18 (d, $J$ = 7.9 Hz, 1H); 7.25 (m, 1H); 7.41 (m, 1H); 7.65 (m, 1H); 7.78 (d, $J$ = 4.8 Hz, 1H); 7.82 (td, $J$ = 7.7, 1.7 Hz, 1H); 8.74 (d, $J$ = 4.7 Hz, 1H). The ratio of the isomers is 93:7 after 24 h. In the spectrum of the major isomer, the appearance of one singlet at 2.04 ppm, corresponding to the *p*-tolyl methyl protons, and a broad singlet at 8.64 ppm, corresponding to the 5-pyridyl protons, confirms the magnetic equivalence of similar protons in this complex and is consistent with $C_2$ or $C_s$ symmetry. The minor isomer shows two singlets at 2.11 and 1.95 ppm, corresponding to the *p*-tolyl methyl protons, and two doublets at 8.74 and 7.78 ppm, corresponding to the 5-pyridyl protons. This result confirms the magnetic inequivalence of similar protons in this isomer and is consistent with $C_1$ symmetry. Anal. Calcd for $C_{34}H_{40}N_6O_2PF_6ClZn_2$: C, 46.62; H, 4.61; N, 9.60; Cl, 4.05. Found: C, 46.70; H, 4.60; N, 9.51; Cl, 3.79.

**[Zn(enenam)Zn](PF$_6$)$_2$.** $^1$H NMR (400 MHz, acetone-$d_6$): major isomer, $\delta$ 2.07 (s, 6H); 3.22 (m, 2H); 3.42 (m, 2H); 3.60 (m, 4H); 4.06 (m, 4H); 4.34, 4.21 (syst AB, $J_{AB}$ = 16.2 Hz, 4H); 4.59, 3.65 (syst AB, $J_{AB}$ = 11.9 Hz, 4H); 6.60 (s, 2H); 6.87 (s, 2H); 7.14 (d, $J$ = 7.9 Hz, 2H); 7.28 (t, $J$ = 6.2 Hz, 2H); 7.68 (td, $J$ = 7.7, 1.7 Hz, 2H); 8.72 (br s, 2H). There is evidence of at least one other isomer at the following positions: minor isomer, $\delta$ 2.01 (s, 3H); 2.14 (s, 3H); 6.48 (s, 1H); 6.82 (d, $J$ = 1.9 Hz, 1H); 6.84 (d, $J$ = 1.7, 1H); 7.01 (s, 1H); 7.15 (m, 1H); 7.29 (m, 3H); 7.47 (m, 1H); 7.74 (m, 1H); 7.86 (td, $J$ = 7.8, 1.5 Hz, 1H); 8.72 (br s, 1H). The ratio of isomers is 90:10 after 24 h. In the spectrum of the major isomer, the appearance of one singlet at 2.07 ppm, corresponding to the *p*-tolyl methyl protons, and one broad singlet at 8.72 ppm, corresponding to the 5-pyridyl protons, confirms the magnetic equivalence of similar protons in this isomer, and is consistent with $C_2$ or $C_s$ symmetry. The minor isomer shows two singlets at 2.14 and 2.01 ppm, corresponding to the *p*-tolyl methyl protons, and two resonances at 8.72 and 7.74 ppm, corresponding to the 5-pyridyl protons. This result is consistent with $C_1$ symmetry.

**[Co(diamine)CoCl](PF$_6$)$_2$ Complexes. [Co(tntnam)CoCl](PF$_6$)$_2$·H$_2$O.** All prodecures were carried out under Ar using deaerated solvents and standard Schlenk techniques. To a stirred solution of [Co(tntnam)(H$^+$)$_2$](PF$_6$)$_3$ (250 mg, 0.230 mmol) and $CoCl_2$·6$H_2O$ (55.8 mg, 0.230 mmol) in acetone (5 mL) was added dropwise over 5 min LiOH·$H_2O$ (19.7 mg, 0.460 mmol) in methanol (5 mL). The resultant dark maroon solution was stirred for 5 min, and then $NH_4PF_6$ (95 mg, 0.58 mmol) in methanol (5 mL) was added to it. The reaction mixture was stirred for 30 min, and then was concentrated to dryness under high vacuum (<0.25 mm Hg). The solid was slurried in a mixture of 50:50 $Et_2O$−ethanol (5 mL) to remove colored (green) impurities. The black solid was collected, washed with ethanol (3 × 5 mL, no color was observed in the final wash), and dried under high vacuum. The crude product (201.5 mg, 84%) was recrystallized from $CH_3CN$−EtOH−$Et_2O$ in the same manner as the monometallic Co(III) complexes. Yield: 45%. The product was found to be air stable as a solid and in solution, based on the constancy of the electronic spectrum over 24 h. $\Lambda_m$ = 264 $\Omega^{-1}$ mol$^{-1}$ cm$^2$. UV: 434 (5700), 568 (2530), 1098 (8). Anal. Calcd for $Co_2C_{36}H_{44}N_6O_2P_2F_{12}Cl$·$H_2O$: C, 41.02; H, 4.41; N, 7.97; Cl, 3.36. Found: C, 40.70; H, 4.15; N, 7.89; Cl, 3.22. The IR spectrum closely resembles that of [Zn(tntnam)ZnCl]PF$_6$, except for the presence of a broad band at 3440 cm$^{-1}$ and significant broadening of the band at 1611 cm$^{-1}$. Both of these additional features are consistent with the retention of water in the crystalline material.[24]

**[Co(tnenam)CoCl](PF$_6$)$_2$.** All procedures were carried out in air. To a stirred solution of [Co(tnenam)(H$^+$)$_2$](PF$_6$)$_3$ (25.5 mg, 0.0237 mmol) and $CoCl_2$·6$H_2O$ (5.76 mg, O.0237 mmol) in acetone (1 mL)

was added $LiOH \cdot H_2O$ (2.03 mg, 0.0475 mmol) in methanol (1 mL). The resultant dark maroon solution was stirred for 5 min, and then $NH_4PF_6$ (10 mg, 0.059 mmol) in methanol (1 mL) was added. The reaction mixture was stirred for 30 min, and then was concentrated to dryness on a rotary evaporator. The resultant solid was slurried in 50:50 $Et_2O$−ethanol (2 mL), collected, and washed with ethanol (2 × 1 mL), $Et_2O$ (3 × 1 mL), and pentane (3 × 1 mL). The crude product (10.7 mg, 44%) was not purified further. The electronic spectrum was recorded in $CH_3CN$. The extinction coefficents were calculated using the formula for $[Co(tnenam)CoCl](PF_6)_2$, and may therefore be underestimated if impurities were present. UV: 425 (2800), 549 (1100), 1098 (6).

**$[Co(entnam)CoCl](PF_6)_2$.** The complex was prepared by the same method used for the preparation of $[Co(tnenam)CoCl](PF_6)_2$. The crude product was recrystallized from $CH_3CN-EtOH-Et_2O$ in the same manner as for the monometallic Co(III) complexes. Yield: 26%. $\Lambda_m = 274\ \Omega^{-1}\ mol^{-1}\ cm^2$. UV: 414 (4000), 560 (1000), 819 (16), 1041 (10). The extinction coefficents were calculated using the formula for $[Co(entnam)CoCl](PF_6)_2$, which is supported by the conductivity measurements, although solvents of crystallization may be present.

**$[Co(diamine)CoCl]PF_6$ Complexes.** The dicobalt(II) complexes were prepared by the general method described for $[Co(tnenam)CoCl]PF_6$, which is the only such complex that was obtained in analytically pure form. These complexes are considerably more air-sensitive than their monometallic precursors, and rigorous adherence to Schlenk techniques was necessary for their preparation.[26] All complexes show a ligand-based absorption in the electronic spectrum at $\lambda_{max} = 300$ nm ($\epsilon = 5500-6500\ L\ mol^{-1}\ cm^{-1}$) in $CH_3CN$ solutions.

**$[Co(tnenam)CoCl]PF_6$.** To a stirred solution of $[Co(tnenam)(H^+)_2](PF_6)_2$ (429.1 mg, 0.461 mmol) and $CoCl_2 \cdot 6H_2O$ (115.1 mg, 0.474 mmol) in acetone (2.5 mL) was added dropwise over 5 min $LiOH \cdot H_2O$ (39.9 mg, 0.951 mmol) in methanol (5 mL). The resultant dark red solution was stirred for 15 min. The solution was filtered to remove the small amount of fluffy precipitate that had formed, and then $NH_4PF_6$ (190 mg, 1.15 mmol) in methanol (5 mL) was added to it. The reaction mixture was then concentrated to dryness. The pink residue was slurried in ethanol (10 mL) to remove dark-colored impurities. The solid was collected, washed with ethanol (2 × 10 mL), and dried under high vacuum (<0.25 mm) for 4 h. The crude product was recrystallized as follows. The crude $[Co(tnenam)CoCl]PF_6$ complex (175 mg) was dissolved in acetone (0.75 mL) and the solution was filtered. The residue was washed through the filter with acetone (0.75 mL). The resultant solution was diluted with ethanol (10 mL). Precipitation began almost immediately. Further aliquots of ethanol (10 mL) were added to the mixture after 30 min and 1 h. The solid was then collected, washed with ethanol (3 × 10 mL), and dried under high vacuum (<0.25 mm) for 2 h. The $[Co(tnenam)CoCl]PF_6$ complex was obtained as a microcrystalline magenta solid (100 mg, 57% recovery). $\Lambda_m = 119\ \Omega^{-1}\ mol^{-1}\ cm^2$. UV: 453 (70), 498 (65), 544 (42), 613 (23), 647 (20), 666 (17), 692 (12), 964 (5). Anal. Calcd for $Co_2C_{35}H_{42}N_6O_2PF_6Cl$: C, 47.82; H, 4.84; N, 9.58; Cl, 4.04. Found: C, 47.67; H, 4.84; N, 9.35; Cl, 3.70.

**$[Co(tntnam)CoCl]PF_6$.** The crude product was washed with $H_2O$ instead of ethanol, due to its significant solubility in the latter. The crude product could not be purified further. Yield: 85%. UV: 480 (71), 530−585 (45), 625−680 (25), 795 (2), 997 (6), 1190−1280 (3). The extinction coefficents were calculated using the formula for $[Co(tntnam)CoCl]PF_6$, and may be underestimated if impurities are present.

**$[Co(entnam)CoCl]PF_6$.** The crude product was washed with $H_2O$ instead of ethanol, and could not be purified further. Yield: 81%. The electronic spectrum was obscured by the Co(III)−phenolate charge transfer band and by Co(III) d−d bands associated with traces of oxidized material in the sample which precluded reliable band assignments.

**Reactivity Studies with $[Co(diamine)CoCl](PF_6)_n$ ($n$ = 1, 2) Complexes. 1. Reactions with $NOPF_6$.** All reactions were done under Ar using standard Schlenk techniques.

**$[Co(tntnam)CoCl]PF_6 + NOPF_6$.** To a stirred red-purple solution of $[Co(tntnam)CoCl]PF_6$ (101 mg, 0.112 mmol) in propionitrile (2.5 mL) at −78 °C was added $NOPF_6$ (30 mg, 0.17 mmol) in propionitrile (2.5 mL, precooled to −78 °C). The resultant green-black solution was warmed to room temperature and then concentrated to dryness. The black residue was slurried in a 1:1 $Et_2O$−ethanol mixture (6 mL), to remove colored (brown) impurities. The solid was collected, washed with $Et_2O$ (3 × 5 mL), and then dried under vacuum. The solid was recrystallized from $CH_3CN$−ethanol−$Et_2O$ in the same manner as the monometallic cobalt(III) complexes. The product was obtained as a green microcrystalline solid (58.4 mg). The IR spectrum shows no N≡O stretch. The IR and electronic spectra are identical to those of the authentic $[Co(tntnam)CoCl](PF_6)_2$ complex. To a solution of the purified product (50 mg) in $CH_3CN$ (2.5 mL) in a small evaporating dish was added $NH_4PF_6$ (100 mg, 0.61 mmol) in ethanol (2.5 mL), followed by water (10 mL). The resultant green solution was heated on the steam bath for approximately 20 min. Black needles precipitated from the mixture as the solvents were evaporated. The crystals were collected, washed with water (2 × 5 mL), and dried under vacuum. Yield: 12 mg. A $^1H$ NMR spectrum was identical with that of the $[Co(tntnam)(H^+)_2](PF_6)_3$ complex.

**$[Co(tnenam)CoCl]PF_6 + NOPF_6$.** The reaction was run by the same method described for $[Co(tntnam)CoCl]PF_6$, except that the reagents were mixed in $CH_3CN$ at −35 °C, instead of propionitrile at −78 °C. The IR spectrum shows no N≡O stretch. UV: 432 (1800), 567 (800), 955 (4). The sample was heated on the steam bath by the described procedure and a crystalline product was obtained. The $^1H$ NMR spectrum of this product was identical to that of the $[Co(tnenam)(H^+)_2](PF_6)_3 \cdot CH_3CN$ complex.

**$[Co(entnam)CoCl]PF_6 + NOPF_6$.** The reaction was run by the method described for $[Co(tntnam)CoCl]PF_6$. The IR spectrum shows no N≡O stretch. The electronic spectrum shows clear bands at 419 (1540) and 561 (535). The 900−1200-nm region is complicated by overlapping bands, but intensity is detected at approximately 1040 nm and is attributed to O-site cobalt(II) by comparison with the authentic $[Co^{III}(entnam)Co^{II}Cl](PF_6)_2$ complex. The sample was heated on the steam bath by the described procedure, and a crystalline solid was obtained. The $^1H$ NMR spectrum of this product was identical with that of the $[Co(entnam)(H^+)_2](PF_6)_3$ complex.

**2. Reactions with $O_2$. $[Co(tntnam)CoCl]PF_6 + O_2$.** The $[Co(tntnam)CoCl]PF_6$ complex (75.5 mg, 0.0847 mmol) was dissolved in $CH_2Cl_2$ (3.4 mL) forming a magenta solution. Air was then bubbled through the solution for 10 min. The resultant dark maroon solution was allowed to stand in air for 24 h. UV ($CH_2Cl_2$): 445 (1800), 566 (800), 960 (6). To this solution was added acetic acid (4.86 $\mu$L, 0.0847 mmol). After 5 days, the electronic spectrum was unchanged. The reaction mixture was concentrated to dryness. The residue was taken up in $CH_3CN$ (5 mL) and heated on the steam bath for 10 min. The mixture was concentrated to dryness. The residue was no longer fully soluble in $CH_2Cl_2$. A spectrum of a uniform sample in $CH_3CN$ was taken. UV ($CH_3CN$): 435 (1800), 566 (800), 960 (6). The shift in the charge transfer band at 435 nm appears to be a solvent effect. The solution was concentrated to dryness. The residue was reacted with $[Cp_2Fe]PF_6$ (28 mg, 0.085 mmol) by the method described for the preparation of $[Co(tntnam)(H^+)_2](PF_6)_3$. No $[Cp_2Fe]$ was produced. The spectrum of the crude product (39.0 mg) was somewhat obscured by the strong charge transfer bands associated with the residual $[Cp_2Fe]PF_6$. The material was recrystallized from $CH_3CN-EtOH-Et_2O$. The purified product was obtained as a fluffy dark green solid (20 mg). The UV spectrum in $CH_3CN$ was identical to that of the authentic $[Co(tntnam)CoCl](PF_6)_2$ complex. The sample was heated on the steam bath by the procedure described under the reaction of $[Co(tntnam)CoCl]PF_6 + NOPF_6$. A $^1H$ NMR spectrum of the crystalline product was identical with that of the $[Co(tntnam)(H^+)_2](PF_6)_3$ complex. The reaction was repeated and the residue obtained after only prolonged air exposure was heated on the steam bath by the described procedure with excess $NH_4PF_6$. The resultant product also showed a $^1H$ NMR spectrum that was identical to that of the $[Co(tntnam)(H^+)_2](PF_6)_3$ complex.

**$[Co(tnenam)CoCl]PF_6 + O_2$.** The $[Co(tnenam)CoCl]PF_6$ complex (74.5 mg, 0.0849 mmol) was dissolved in $CH_2Cl_2$ (3.40 mL) forming a magenta solution. Air was then bubbled through the solution for 10 min. The resultant dark maroon solution was allowed to stand in air. After 3 h, crystals began to form. The solution was left for 24 h as

(26) Shriver, D. F.; Drezdzon, M. A. *The Manipulation of Air-Sensitive Compounds*, 2nd ed.; John Wiley & Sons: New York, 1986.

the $CH_2Cl_2$ was allowed to evaporate slowly. The crystals were then collected, washed with $CH_2Cl_2$ (2 × 2 mL) and pentane (2 × 2 mL), and then dried under vacuum for 5 min. Yield: 11.0 mg. UV ($CH_3CN$): 449 (1000), 619 (340), 1004 (18). The electronic spectrum of the filtrate was identical in the 400−1200-nm region. The crystals and the filtrate were independently heated on the steam bath by the procedure described under the reaction of [Co(tntnam)CoCl]$PF_6$ + $NOPF_6$. The $^1$H NMR spectrum of each of the products was identical with that of the [Co(tnenam)$(H^+)_2$]$(PF_6)_3$ complex.

**[Co(entnam)CoCl]$PF_6$ + $O_2$.** The [Co(entnam)CoCl]$PF_6$ complex (107.5 mg, 0.123 mmol) was dissolved in $CH_2Cl_2$ (5 mL) at 0 °C forming a magenta solution. Air was then bubbled through the solution for 10 min. The resultant dark maroon solution was allowed to stand in air for 1 h. A tacky black precipitate formed as the $CH_2Cl_2$ evaporated. To this mixture was added acetic acid (7.0 $\mu$L, 0.12 mmol). The precipitate dissolved immediately. To the resultant solution was added $NH_4PF_6$ (100 mg, 0.613 mmol) in ethanol (2.5 mL). As the solvents were allowed to evaporate over 24 h, a black precipitate formed. When most of the color had vanished from the remaining solution (at 24 h, with a volume of approximately 1 mL), the solid was collected, washed with ethanol (1 × 5 mL), $Et_2O$ (2 × 3 mL), and pentane (2 × 3 mL), and dried under vacuum. The crude product (98.1 mg) was recrystallized from $CH_3CN$−ethanol−$Et_2O$ in the same manner as the monometallic cobalt(III) complexes. Yield: 33.9 mg. The electronic spectrum of the purified product was identical to that of the crude product. $\Lambda_m = 286\ \Omega^{-1}\ mol^{-1}\ cm^2$. UV ($CH_3CN$): 411 (1900), 559 (560), 979 (6). The infrared spectrum of the product is very similar to those of [Zn(tntnam)ZnCl]$PF_6$ and [Co(tntnam)CoCl]$(PF_6)_2$. The significant differences include the emergence of a band at 2260 $cm^{-1}$, which is attributed to the C≡N stretch of acetonitrile retained in the crystal,[24] and the emergence of a strong band at 1600 $cm^{-1}$, which is attributed to the C═O stretch of a coordinated acetate. A similar band was observed at 1593 $cm^{-1}$ in the spectrum of [Zn(tntnim)Zn(OAc)]-$PF_6$.[7] The product was therefore formulated as [Co(entnam)Co-(OAc)($CH_3CN$)]$(PF_6)_2$. Anal. Calcd for $Co_2C_{37}H_{45}N_6O_4P_2F_{12}$·$CH_3CN$: C, 43.10; H, 4.46; N, 9.02; Co, 10.84; Cl, 0. Found: C, 43.31; H, 4.65; N, 8.93; Co, 11.06; Cl, 0.14. The product was heated on the steam bath with excess $NH_4PF_6$ by the described procedure. A $^1$H NMR spectrum of the resultant crystals was identical with that of the [Co(entnam)$(H^+)_2$]$(PF_6)_3$ complex.

**3. Reactions with [$Cp_2Fe$]$PF_6$.** All reactions were done under Ar using standard Schlenk techniques.

**[Co(tntnam)CoCl]$PF_6$ + 2[$Cp_2Fe$]$PF_6$.** To a stirred solution of [Co(tntnam)CoCl]$PF_6$ (75.2 mg, 0.0844 mmol) in propionitrile (2.5 mL) at −78 °C was added [$Cp_2Fe$]$PF_6$ (58.4 mg, 0.176 mmol) in propionitrile (2.5 mL, precooled to −78 °C). The resultant green-black solution was warmed to room temperature and was then concentrated to dryness. The black residue was triturated with $Et_2O$ (3 × 5 mL) to remove $Cp_2Fe$. The $Et_2O$ washes were combined and concentrated to dryness, yielding $Cp_2Fe$ (12.9 mg, 0.0800 mmol). The remaining black solid was collected and washed with a 1:1 mixture of $Et_2O$−EtOH (3 × 5 mL), EtOH (3 × 5 mL), and $Et_2O$ (3 × 3 mL), and then it was dried under vacuum. The crude product was obtained as a black powder (68.9 mg). The UV spectrum shows d−d bands from residual [$Cp_2Fe$]$PF_6$ overlapping with the cobalt(III) d−d bands in the region near 560 nm, and is otherwise identical to that of the authentic [Co(tntnam)CoCl]-$(PF_6)_2$ complex. The crude product was heated on the steam bath by the procedure described under the reaction of [Co(tntnam)CoCl]$PF_6$ + $NOPF_6$, except the heated solution was filtered through Celite twice to remove insoluble material derived from the residual [$Cp_2Fe$]$PF_6$. A $^1$H NMR spectrum of the crystalline product was identical with that of the [Co(tntnam)$(H^+)_2$]$(PF_6)_3$ complex.

**[Co(tnenam)CoCl]$PF_6$ + 2[$Cp_2Fe$]$PF_6$.** To a stirred magenta solution of [Co(tnenam)CoCl]$PF_6$ (42.0 mg, 0.048 mmol) in $CH_3CN$ (1.4 mL) was added [$Cp_2Fe$]$PF_6$ (16.0 mg, 0.048 mmol) in $CH_3CN$ (1 mL). The reaction mixture turned deep burgundy. The solution was stirred 5 min. The electronic spectrum of the resultant mixture was identical to that of the authentic [Co(tnenam)CoCl]$(PF_6)_2$ complex. To this mixture was added [$Cp_2Fe$]$PF_6$ (16 mg, 0.048 mmol) in $CH_3CN$ (1 mL). The reaction mixture was stirred 5 min. The electronic spectrum was unchanged. The reaction mixture was concentrated to dryness. The residue was heated on the steam bath by the procedure described under the reaction of [Co(tntnam)CoCl]$PF_6$ + 2[$Cp_2Fe$]$PF_6$. A $^1$H NMR spectrum of the crystalline product was identical with that of [Co(tnenam)$(H^+)_2$]$(PF_6)_3$.

**[Co(entnam)CoCl]$PF_6$ + 2[$Cp_2Fe$]$PF_6$.** The reaction was run by the method described for [Co(tntnam)CoCl]$PF_6$ + 2[$Cp_2Fe$]$PF_6$. The electronic spectrum is identical to that of the authentic [Co(entnam)-CoCl]$(PF_6)_2$ complex. The sample was heated on the steam bath by the described method. A $^1$H NMR spectrum on the crystalline product was identical to that of the [Co(entnam)$(H^+)_2$]$(PF_6)_3$ complex.

**[Co(entnam)Co($CH_3CN$)(OAc)]$(PF_6)_2$ + [$Cp_2Fe$]$PF_6$.** To a stirred solution of [Co(entnam)Co($CH_3CN$)(OAc)]$(PF_6)_2$ (44.5 mg, 0.0409 mmol) in $CH_3CN$ (4.1 mL) was added [$Cp_2Fe$]$PF_6$ (13.8 mg, 0.0409 mmol) in $CH_3CN$ (1.5 mL). The resultant solution was stirred for 10 min. The electronic spectrum of this material was unchanged, except for the presence of transitions associated with [$Cp_2Fe$]$PF_6$.

**X-ray Structure Determinations.** Crystallographic data for both complexes are collected in Tables 1 and 4. Both the red, plate-like crystals of [Co(tnenam)$(H^+)_2$]$(PF_6)_3$·$CH_3CN$, **I**, and the colorless crystals of [Zn(enenam)ZnCl]$PF_6$, **II**, were photographically characterized and both were determined to belong to the monoclinic crystal system. Systematic absences in the diffraction data uniquely determined the space group for each complex. The asymmetric group in **II** contains two independent molecules. In each case, azimuthal scans indicated that no correction for absorption was required; $T_{max}/T_{min} < 1.1$. Each structure was solved by direct methods, completed from difference Fourier maps, and refined with anisotropic thermal parameters for all non-hydrogen atoms. Hydrogen atom contributions were idealized except for those associated with O(1), O(2), N(5), and N(6) in structure **I**, which were ignored due to uncertainties in their location. All computations used SHELXTL 4.2 software (G. Sheldrick, Siemens XRD, Madison, WI).

**Acknowledgment.** This work was supported by grants from the National Science Foundation.

**Supporting Information Available:** Top and side views of the second molecule in the asymmetric group of structure **II**, and tables of detailed crystallographic data for **I** and **II**, including crystal and structure refinement data, atomic coordinates, complete bond distances and angles, anisotropic displacement parameters, hydrogen coordinates and isotropic displacement parameters (24 pages); tables of observed and calculated structure factors (42 pages). This material is contained in many libraries on microfiche, immediately follows this article in the microfilm version of the journal, can be ordered from the ACS, and can be downloaded from the Internet; see any current masthead page for ordering information and Internet access instructions.

JA952873C